Sudan University of Science and Technology

College of Graduate Studies

Evaluation of Patient Radiation Dose During Computed Tomography Angiography

تقويم جرعة الأشعة للمريض أثناء فحص الأوعية الدموية بواسطة الأشعة المقطعية

A thesis submitted for partial fulfillment of the Requirements of the M.SC Degree in Diagnostic Radiological Technology

By:

Khawla Hassan Abass Ahmed

Supervisor:

Dr. Hussein Ahmad Hassan

2016

بسم الله الرحمن الرحيم

الآية

قال تعالى:

) قالوا سبحانك لا علم لنا إلا ما علمتنا إنك أنت العليم الحليم)

الآية 32 من سورة البقرة

Dedication

Every challenging work needs self-efforts as well as

Guidance of elders especially those who were very close to

our heart.

To those of the fingers to give us a life of happiness.
My humble effort I dedicate to my sweet and lovely

Mother.

To reap the thorns out of my way for me to pave the way science
To the great heart my father.

Whose affection, love, encouragement, and prays of day and

Night make me able to get such success and honor,

Along with all hard working and respected teachers

To my brother, friends, and to all my family.

Acknowledgements

First and foremost, I would like to express my deepest gratitude to Dr. **Hussein Ahmed Hassan** for his support and guidance. Without his help this work could not have been accomplished.

I also would like to thank Dr. Mohammed Elfadil Mohammed for his contribution in this research.

My thanks also go to Royal Scan Diagnostic Center staff for their help.

Deep thanks to my friends. Finally, I would like to sincerely thank my family for their consistent mental support.

ABSTRACT

Computed Tomography (CT) is a diagnostic imaging modality giving higher patient dose in comparison with other radiologic procedures, so the calculation of patient dose in CT exams is very important. CT improved many diagnoses of diseases. The increasing use of CT in Sudan in recent years is what has to think in the attempt to reduce the exposure of the patient and that the risks known to the X-ray. This study aimed to assess the radiation dose and estimating the risks resulting from exposure to X-rays during CT angiography (CTA).

A total of 50 patients were examined in Royal Scan Diagnostic Center using spiral CT scans 64 slices (in the period September 2015-December 2015). The average age of the samples was (45.0±82.0) years. The mean effective dose per procedure was (51.6±15.3mSv), (31.5±10.0mSv), (74.5±16.8mSv) for the renal, coronary and lower limb respectively. Patients are exposed to a considerable dose during the procedures. Patient dose during limbs procedures are higher compared to the other two examinations.

الملخص

الأشعة المقطعية هي تقنية تصوير طبي ،عند إستخدامها تعطي جرعة إشعاع عالية للمريض بالمقارنة مع الفحوصات الإشعاعية الأخرى، لذلك حساب الجرعات الإشعاعية للمرضى مهم جدا. كما أن الأشعة المقطعية زادت من المقدرة على تشخيص كثير من الأمراض. تُعتبر زيادة إستخدام الأشعة المقطعية في السودان في السنوات الأخيرة من الأسباب التي حفزت الباحثين لخفض الجرعة الإشعاعية والخطر الإشعاعي المصاحب. لذلك هدفت هذه الدراسة إلى قياس الإشعاع وتقدير الخطر الإشعاعي الناجم عن فحوصات الأشعة المقطعية للأجهزة ذات الأربعة وستون شريحة.

تم فحص 50 مريضا بمركز رويال سكان التشخيصي في الفترة من سبتمبر و حتى ديسمبر 2015. بلغ متوسط العمر للمرضى (45.0±82.0) سنة. بلغ متوسط الجرعة الفعالة للأوعية الدموية لكل من الكلي و القلب و الأطراف السُفلى (51.6±15.3ملي سيفرت) , (31.5±10.0ملي سيفرت) , (74.5±16.8ملي سيفرت)علي التوالي.
يتعرض المريض لجرعة معتبرة اثناء فحص الاوعية الدموية بالاشعة المقطعية. الجرعة الاشعاعية للاطراف اعلي بالمقارنة مع بقية الفحوصات.

List of Abbreviations

CTDI	Computed Tomography Dose Index
DLP	Dose Length Product
MSAD	Multi Scan Arrange Dose
CTA	Computed Tomography Angiography
MPR	Multi Planar Reformation
MIP	Maximum Intensity Projection
CCTA	Coronary Computed Tomography Angiography
ALARA	As Low As Reasonably Achievable
MSCT	Multi Slice Computed Tomography

List of Figures

List of Tables

Table of Contents

CHAPTER ONE:

1.1 Historical review of CT:

The earliest CT scanner, developed by Sir Godfrey Hounsfield, and independently developed by Allen Cormack, was first used for brain imaging in 1972. Each single homographic slice required hours of scan time and days of computation to render what was a truly revolutionary image of skull, brain, and cerebrospinal fluid. These early CT images were remarkable because for the first time, the soft tissues within the skull could be visualized with both contrast and spatial resolution that was not possible with other topographic techniques. Advances during the next 2 decades led to scanners that were faster and could achieve even better contrast and spatial resolution. Nevertheless, by the mid-1980s, CT scanners still worked the same way, obtaining each image slice-by-slice, with incremental table movement followed by circular revolution of the x-ray tube/detector array gantry once around the patient for each image. CT scanning was slow and provided a series of relatively thick and discontinuous slices through the body.(Willmann JK, Mayer D,et al 2003).

The early 1990s saw the introduction of the first helical CT scanners into clinical practice, using a slip-ring mechanism that allowed the x-ray tube/detector array gantry to rotate continuously while the patient was moved smoothly into the scanner. The image data set was therefore a continuous spiral through the patient. Because scanning was continuous, study times were much shorter than comparable studies obtained with non-helical scanners. Still, early helical scanners were not fast enough for many CTA applications. Limitations to faster speed and thinner slice collimation included single-row detector technology (that allowed only one image per gantry rotation), x-ray tubes that were not designed to

handle the intense heat generated during continuous scanning, and computers that were not able to process image data quickly. CT angiography had arrived, but only in very limited applications (Willmann JK, Mayer D,et al 2003).

Toward the mid-1990s, computers had advanced to the point that large image data sets could be reconstructed into a CTA image using a dedicated workstation. X-ray tube technology had also advanced, with the production of tubes that could withstand the amount of heat loading that was generated during continuous x-ray production. However, scanners were still too slow for most angiographic studies because only one image was obtained during gantry rotation, and most gantry spin times had reached a lower threshold of .5 second to 1 second. The only way to scan quickly with a single-detector CT was to use unacceptably thick collimation, or “slice thickness,” that reduced the number of images obtained during the study. Thickly collimated images, however, gave poor spatial resolution in the cranial-caudal or Z-axis. (Willmann JK, Mayer D,et al 2003)

This problem was solved in the late 1990s with the advent of multiple rows of detectors so that many images could be acquired during a single helical revolution. Simultaneous acquisition of multiple slices not only led the way to improved Z-axis resolution, but also reduced the scan time and finally allowed scanning through long segments of the body using acceptable volumes of rapidly delivered intravenous contrast. CTA scanning had finally become a reality, although manipulation of the huge image data sets that resulted from these extensive, thin-collimated studies was relatively slow and required purchase of an expensive workstation that was dedicated to the sole task of three-dimensional (3-D) image manipulation. With ongoing workstation advances during the past 5 years (faster computers, increased random access memory, and improved 3-D

software) and high-speed data transfer networks in most imaging environments, affordable and clinically useful CTA has finally been realized. In fact, today most CT scanners are sold with some form of workstation that can be used for 3-D image post processing. In the near future, it is likely that 3-D software and computational power currently located in a dedicated 3-D workstation will reside somewhere within the imaging picture archiving and communication system network so that any volumetric angiographic imaging study (CT, magnetic resonance imaging, rotational angiography) can be reconstructed into an 3-D angiogram simply by retrieving that study from the data archive. Distribution of 3-D images, still a problem today, will likely be solved through advances in both PACS and Web-based technology. (Willmann JK, Mayer D,et al 2003).

As scanners and computers continue to improve, most single-detector array helical CT scanners in the US have been replaced with multi rows detector units. It was predicted in 1998 that by 2003 at least half of the CT scanners in the US would use multi row detector technology, and this has been realized. What was not predicted, however, was the extremely rapid technological development that led to scanners beyond our 1998 imagination. In 2000, a 4-row detector CT scanner was state of the art. By 2001, 8-row scanners were introduced. By 2003, 16-row scanners entered clinical use. 32- and 40-row scanners are common. Today, 64-row detector scanners are common at many sites. Certainly, one of the driving forces for this burst of CT development and purchase has been the capability of CT scanners to perform CTA of both peripheral and coronary arteries. Scanning peripheral arteries from the skull base to the common femoral arteries with collimation of 0.5 mm to 1 mm takes no longer than 12 seconds to 15 seconds on a 64-row detector CT scanner,

and the CTA images are typically superior to those obtained using invasive angiography.(Willmann JK, Mayer D,et al 2003).

1.2 Computerized topographic angiography (CTA):

Also called CT angiography or CTA, is a test that combines the technology of a conventional CT scan with that of traditional angiography to create detailed images of the blood vessels in the body. In a CT scan, x rays and computers create images that show cross-sections, or slices, of your body. Angiography involves the injection of contrast dye into a large blood vessel, usually in your leg, to help visualize the blood vessels and the blood flow within them. When the contrast dye is used to visualize your veins, the study is called a venogram, and when it is used to visualize your arteries, it is known as an arteriogram. CT angiography is similar to a CT scan, but the contrast dye is injected into one of your veins shortly before the x ray image is performed. Because the dye is injected into a vein rather than into an artery, as in traditional angiography, CT angiography could be considered less invasive (Draffner and Hartman,2014).

1.3 Problem of the Study:

Radiation dose measurements are important in order to estimate the possible risks from diagnostic procedure Patients are exposed to a high radiation dose during angiographic CT imaging. Although, the investigation provides valuable diagnostic information for patient accurate diagnosis, patient protection is crucial.

1.4 Objectives:

1.4.1 General Objective:

- To evaluate the patient radiation doses in CTA imaging.

1.4.2 Specific Objectives:

- To estimate the effective dose from CT angiography in daily practice.
- To compare between the dose estimates from imaging of lower limbs, coronary arteries and renal arteries.
- To correlate between mAs and DLP, mAs and CTDIvol and between DLP and effective dose in lower limbs, coronary arteries and renal arteries.

1.5 Thesis outlines:

This thesis is concerned with the assessment of radiation dose for patients during CTA imaging. Accordingly, it is divided into the following chapters:

Chapter one is the introduction to this thesis. This chapter discusses the objectives and scope of work and introduces necessary background. It also provides an outline of the thesis.

Chapter two contains the background material for the thesis. Specifically it discusses the dose for all absorbed dose measurements and calculations. This chapter also includes a summary of previous work performed in this field, anatomy and physiology.

Chapter three describes the materials and a method used to measure dose for CT machines and explains in details the methods used for dose calculation and optimization.

Chapter four presents the results of this study.

Chapter five presents the discussion, conclusion and recommendations.

Chapter Two

Theoretical Background

2 .1 Anatomy and physiology:

The cardiovascular system can be thought of as the transport system of the body. This system has three main components: the heart, the blood vessel and the blood itself. The heart is the system's pump and the blood vessels are like the delivery routes. Blood can be thought of as a fluid which contains the oxygen and nutrients the body needs and carries the wastes which need to be removed (Scanlon and Sanders 2003).

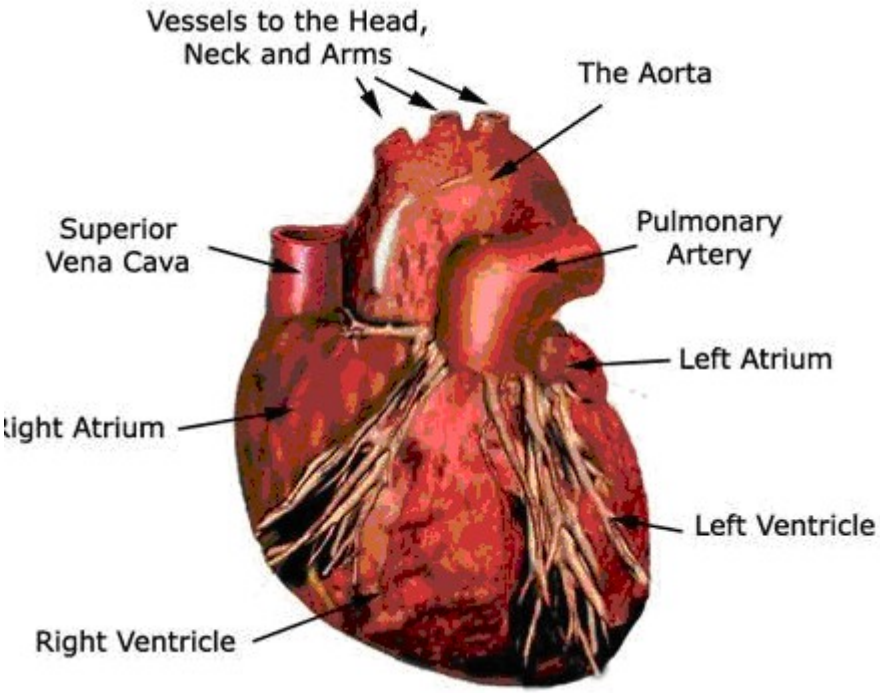

Figure 2.1 shows the anatomy of the heart

(Scanlon and Sanders 2003)

2.1.1 The Cardiovascular System:

The cardiovascular system refers to the heart, blood vessels and the blood. Blood contains oxygen and other nutrients which the body needs to survive. The body takes these essential nutrients from the blood. At the same time, the body dumps waste products like carbon dioxide, back into the blood, so they can be removed. The main function of the cardiovascular system is therefore to maintain blood flow to all parts of the body, to allow it to survive. Veins deliver used blood from the body back to the heart. Blood in the veins is low in oxygen and high in carbon dioxide. All the veins drain into the superior and inferior vena cava which then drains into the right atrium. The right atrium pumps blood into the right ventricle. Then the right ventricle pumps blood to the pulmonary trunk, through the pulmonary arteries and into the lungs. In the lungs the blood picks up oxygen that breathes in and gets rid of carbon dioxide, which breathes out. The blood is becomes rich in oxygen which the body can use. From the lungs, blood drains into the left atrium and is then pumped into the left ventricle. The left ventricle then pumps this oxygen-rich blood out into the aorta which then distributes it to the rest of the body through other arteries. The main arteries which branch off the aorta and take blood to specific parts of the body are:

Carotid arteries, which take blood to the neck and head, Coronary arteries, which provide blood supply to the heart itself, Hepatic artery, which takes blood to the liver with branches going to the stomach, Mesenteric artery, which takes blood to the intestines, Renal arteries, which takes blood to the kidneys and Femoral arteries, which take blood to the legs(Scanlon and Sanders 2003).

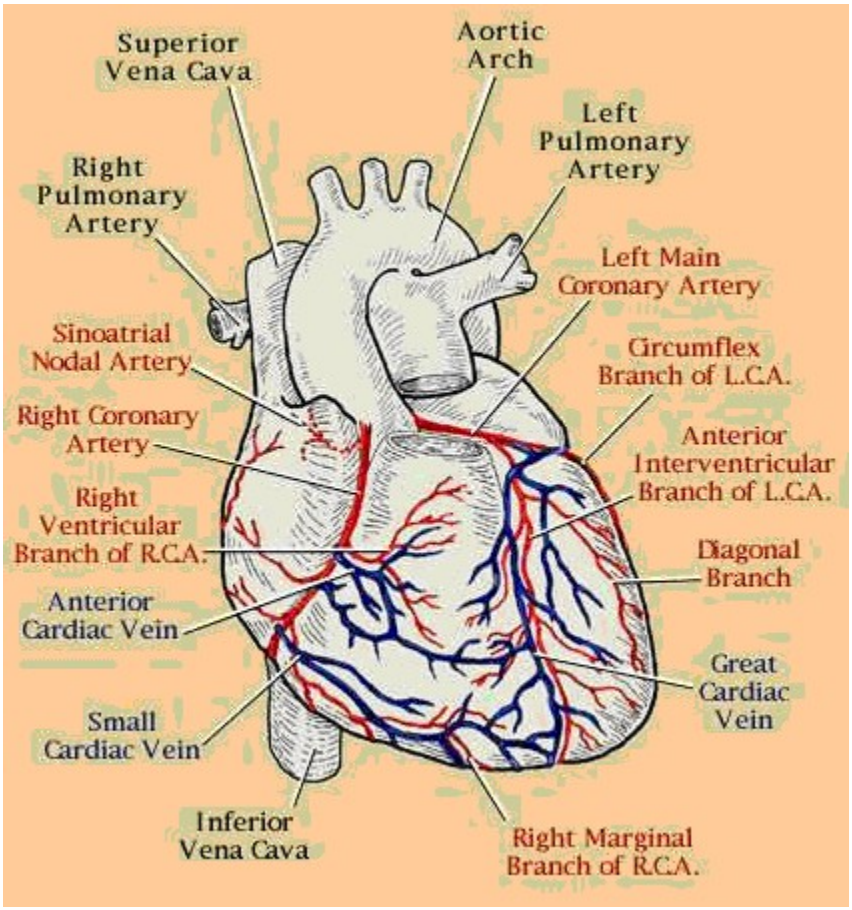

Fig 2.2 shows coronary arteries

(Scanlon and Sanders 2003).

The body is then able to use the oxygen in the blood to carry out its normal functions. This blood will again return back to the heart through the veins and the cycle continues. (Scanlon and Sanders 2003).

2.1.2 Blood Vessels:

Blood Vessel is tubes which carry blood. Veins are blood vessels which carry blood from the body back to the heart. Arteries are blood vessels which carry blood from the heart to the body. There are also microscopic blood vessels which connect arteries and veins together called capillaries. There are a few main blood vessels which connect to different chambers of the heart. The aorta is the largest artery in the body. The left ventricle pumps blood into the aorta which then carries it to the rest of the body

through smaller arteries. The pulmonary trunk is the large artery which the right ventricle pumps into. It splits into pulmonary arteries which take the blood to the lungs. The pulmonary veins take blood from the lungs to the left atrium. All the other veins in the body drain into the inferior vena cava (IVC) or the superior vena cava (SVC). These two large veins then take the blood from the rest of the body into the right atrium. (Scanlon and Sanders 2003).

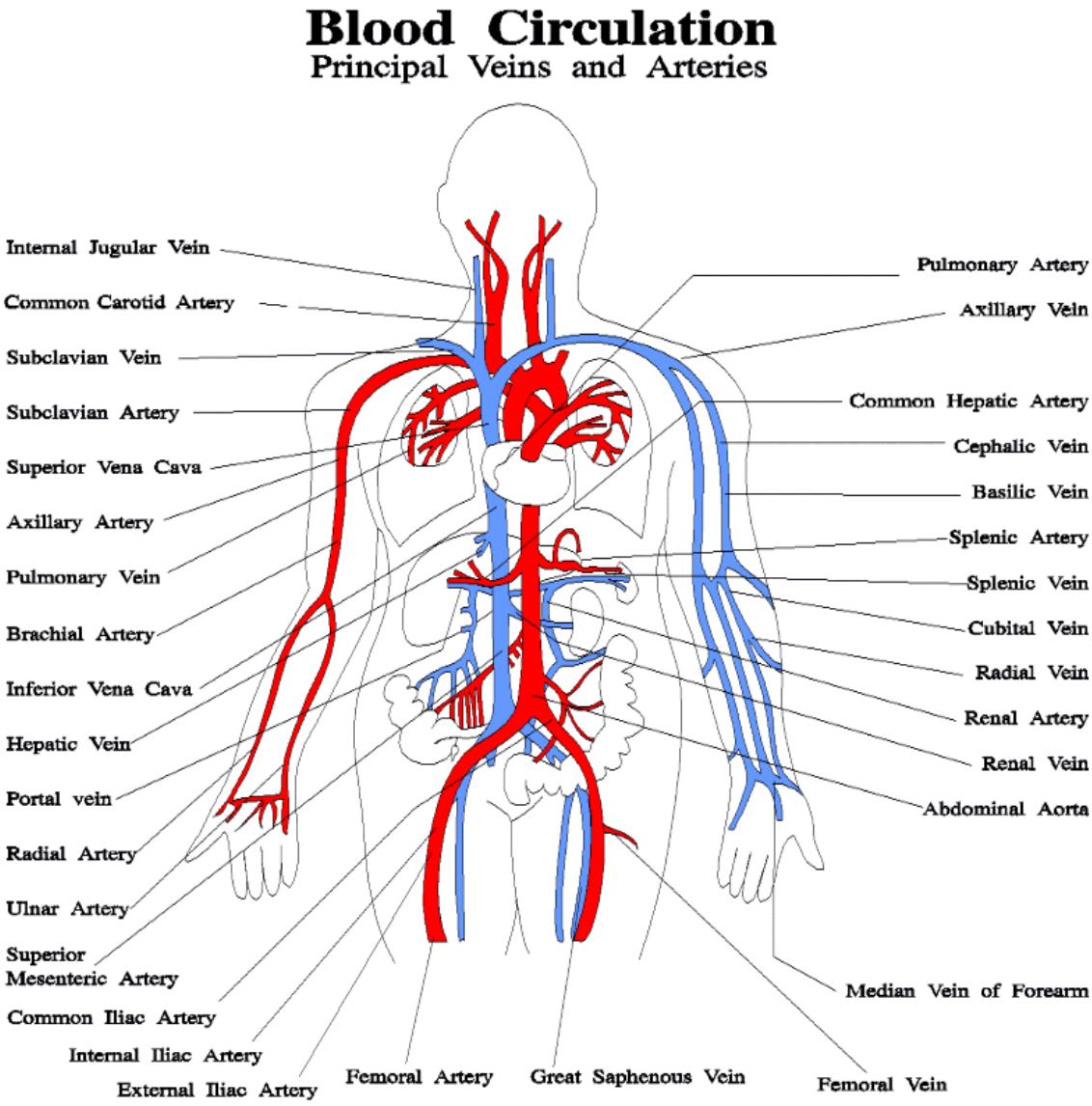

Figure 2.3 shows anatomy of blood vessels

(Scanlon and Sanders 2003).

2.2. Disorders of the Circulatory System:

Hypertension – very high Bp; requires heart to work harder to pump blood damage to blood vessels hemorrhage, stroke; can be caused by arteriosclerosis or hardening of the arteries caused by diets high in cholesterol & saturated fat; fat layers inside vessel walls & it becomes too rigid & lose elasticity also becoming resistant to good blood flow. Stroke – condition results from a blockage in circulation to a part of the brain, Atherosclerosis – result of fatty deposits called plaque lining the walls of the arteries, cholesterol accumulates of the inside of the arterial walls, Hypertension – condition known as high Bp, is related to stress & diets high in salt, Myocardial infarction – term for heart attack condition that occurs when the heart muscle is deprived of O2. Coronary thrombus – a small blood clot becomes lodged in one of the coronary arteries, blocking blood flow to the heart. (Nicholas, Pablo 2005).

2.3 Instrumentation:

The development of computed tomography (CT) in the early 1970s revolutionized medical radiology. For the first time, physicians were able to obtain high-quality topographic (cross-sectional) images of internal structures of the body. Computed topographic images are reconstructed from a large number of measurements of x-ray transmission through the patient (called projection data). The resulting images are topographic "maps" of the x-ray linear attenuation coefficient. A basic system generally consists of a gantry, a patient table, a control console, and a computer. The gantry contains the x-ray source, x-ray detectors, and the data-acquisition system (DAS). (Cunningham,et al. 2000)

2.3.1 Data-Acquisition Geometries

Projection data may be acquired in one of several possible geometries described below, based on the scanning configuration, scanning motions, and detector arrangement. The evolution of these geometries is described in terms of "generations," as illustrated in Fig. 2.4, (Cunningham,et al. 2000)

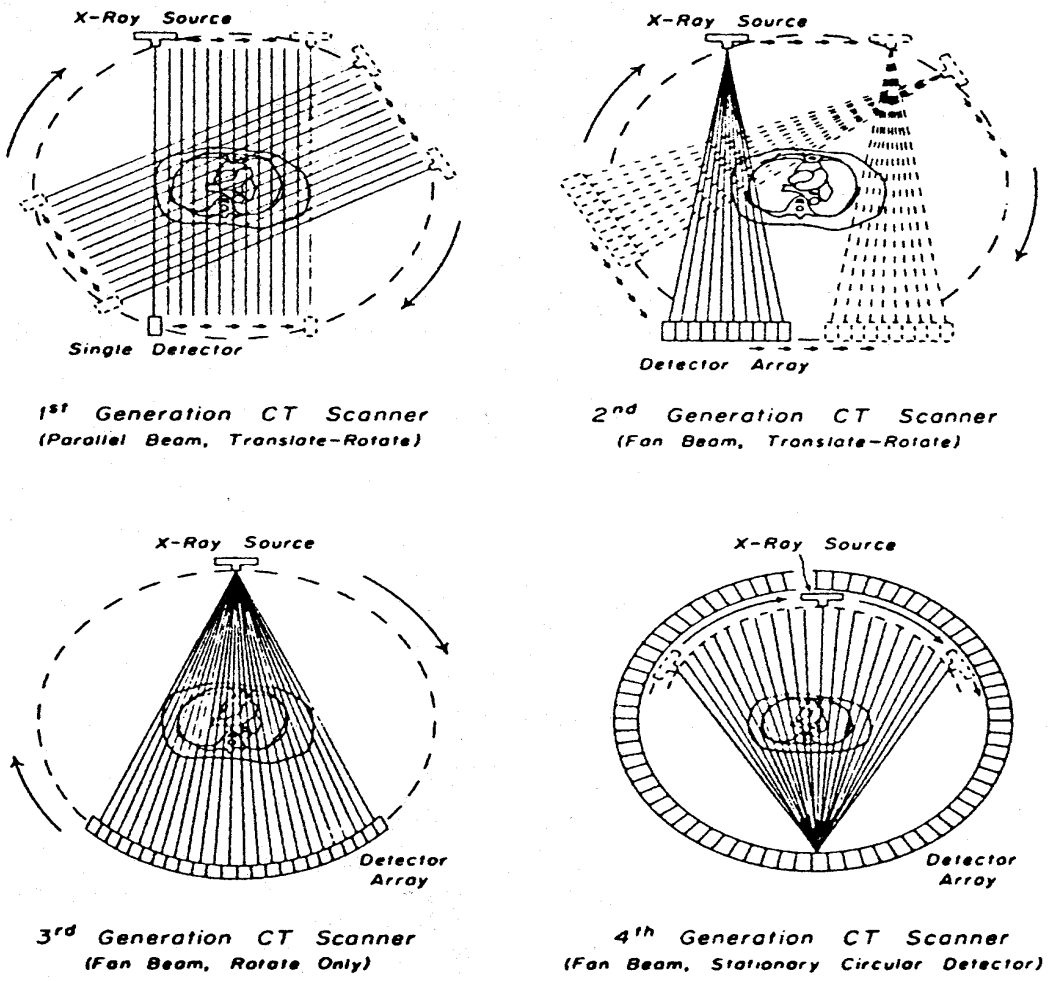

Figure 2.4 Four generations of CT scanners illustrating the parallel- and fan-beam geometries

(Cunningham,et al. 2000)

2.3.1.1 First Generation: Parallel-Beam Geometry:

Parallel-beam geometry is the simplest technically and the easiest with which to understand the important CT principles. Multiple measurements of x-ray transmission are obtained using a single highly collimated x-ray pencil beam and detector. The beam is translated in a linear motion across the patient to obtain a projection profile. The source and detector are then rotated about the patient isocenter by approximately 1 degree, and another projection profile is obtained. This translate-rotate scanning motion is repeated until the source and detector have been rotated by 180 degrees. The highly collimated beam provides excellent rejection of radiation scattered in the patient; however, the complex scanning motion results in long (approximately 5-minute) scan times. (Cunnigham,et.al. 2000).

2.3.1.2 Second Generation: Fan Beam, Multiple Detectors

Scan times were reduced to approximately 30 s with the use of a fan beam of x-rays and a linear detector array. A translate-rotate scanning motion was still employed; however, a larger rotate increment could be used, which resulted in shorter scan times. The reconstruction algorithms are slightly more complicated than those for first-generation algorithms because they must handle fan-beam projection data. (Cunnigham,etal. 2000).

2.3.1.3 Third Generation: Fan Beam, Rotating Detectors

Third-generation scanners were introduced in 1976. A fan beam of x-rays is rotated 360 degrees around the isocenter. No translation motion is used; however, the fan beam must be wide enough to completely contain the patient. A curved detector array consisting of several hundred independent detectors is mechanically coupled to the x-ray source, and

both rotate together. As a result, these rotate-only motions acquire projection data for a single image in as little as 1 s. Third-generation designs have the advantage that thin tungsten septa can be placed between each detector in the array and focused on the x-ray source to reject scattered radiation. (Cunnigham,et.al. 2000).

2.3.1.4 Fourth Generation: Fan Beam, Fixed Detectors:

In a fourth-generation scanner, the x-ray source and fan beam rotate about the isocenter, while the detector array remains stationary. The detector array consists of 600 to 4800 (depending on the manufacturer) independent detectors in a circle that completely surrounds the patient. Scan times are similar to those of third-generation scanners. The detectors are no longer coupled to the x-ray source and hence cannot make use of focused septa to reject scattered radiation. However, detectors are calibrated twice during each rotation of the x-ray source, providing a self-calibrating system. Third-generation systems are calibrated only once every few hours. Two detector geometries are currently used for fourth-generation systems: (A) a rotating x-ray source inside a fixed detector array and (B) a rotating x-ray source outside a notating detector array. Figure 2.5 shows the major components in the gantry of a typical fourth-generation system using a fixed-detector array. Both third- and fourth-generation systems are commercially available, and both have been highly successful clinically. Neither can be considered an overall superior design. (Cunnigham,et.al. 2000).

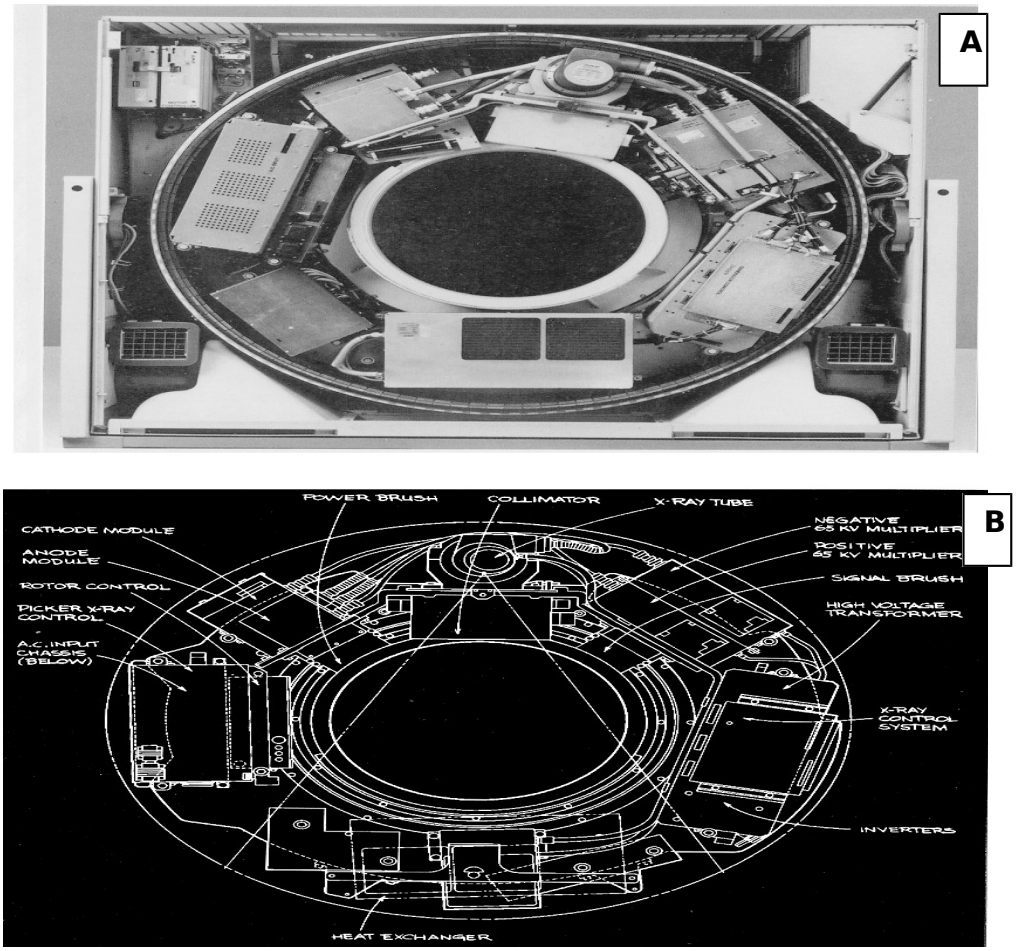

Figures 2.5 A & B show the major components in the gantry of a typical fourth-generation system using a fixed-detector array.

(Cunningham,et al. 2000)

2.3.1.5 Fifth Generation: Scanning Electron Beam:

Fifth-generation scanners are unique in that the x-ray source becomes an integral part of the system design. The detector array remains stationary, while a high-energy electron beams is electronically swept along a semicircular tungsten strip anode. X-rays are produced at the point where the electron beam hits the anode, resulting in a source of x-rays that rotates about the patient with no moving parts (Boyd et al., 1979). Projection data can be acquired in approximately 50 ms, which is fast enough to image the beating heart without significant motion artifacts (Boyd and Lipton, 1983).

An alternative fifth-generation design, called the dynamic spatial reconstructor (DSR) scanner, is in use at the Mayo Clinic (Ritman, 1980, 1990). This machine is a research prototype and is not available commercially. It consists of 14 x-ray tubes, scintillation screens, and video cameras. Volume CT images can be produced in as little as 10 ms.

2.3.1.6 Spiral/Helical Scanning:

The requirement for faster scan times, and in particular for fast multiple scans for three-dimensional imaging, has resulted in the development of spiral (helical) scanning systems (Kalendar et al., 1990). Both third- and fourth-generation systems achieve this using self-lubricating slip-ring technology

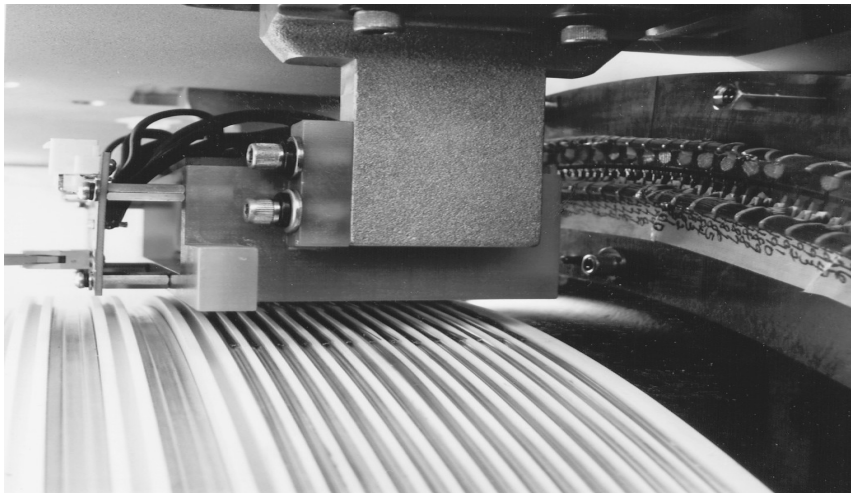

Figure 2.6 Slip ring in CT machine

Photograph of the slip rings used to pass power and control signals to the rotating gantry. (Courtesyof Picker International, Inc.) (Cunningham,et al. 2000)

to make the electrical connections with rotating components. This removes the need for power and signal cables which would otherwise have to be rewound between scans and allows for a continuous rotating motion of the x-ray fan beam. Multiple images are acquired while the patient is translated through the gantry in a smooth continuous motion rather than stopping for each image. Projection data for multiple images

covering a volume of the patient can be acquired in a single breath hold at rates of approximately one slice per second. The reconstruction algorithms are more sophisticated because they must accommodate the spiral or helical path traced by the x-ray source around the patient. (Cunningham,et al. 2000)

2.3.2CT scan machine:

It consists of: The Gantry, The Computer and The Patient couch.

2.3.2.1 The Gantry:

The gantry includes: The x-ray tube,The detector array, The high voltage generator and The collimation.

X-ray Tube; the anode heating capacity must be high, at least several million heat unit (8 MUH), High speed rotators are used for best heat dissipation, Small focal spot size. X-ray tubes are energized with either a continuous or a pulsed x-ray beam.

Special features of x-ray tube internal getters (ion pumps) remove air molecules to ensure a vacuum. Large anode disks e.g. 200 mm (conventional tube disk 120 – 160 mm). The anode disk is thicker than conventional all metal disk. There are three types of disk designs for modern x-ray tubes used in CT. Scanners A) conventional all-metal disk, B) brazed graphite anode disk and C) chemical vapor deposition graphite disk. Slip-Ring Technology Electromechanical devices consisting of circular electrical conductive rings and brushes that transmit electrical energy cross a rotating interface. Design in form of disk or cylinder. Power supply low-voltage or high voltage.

Detector assembly; Early CT scanners had one detector but modern CT scanner have multiple detectors. There is two types of detectors: Scintillation Detector which Convert x-ray to light and Gas Ionization Detector which Convert x-ray energy directly to electrical energy.

X-ray Generator: Three-phase power, High-frequency generator

Collimation: Pre-patient collimator, Post patient or pre-detector collimator. Require for the same reasons as that is required in conventional radiography: Reduce patient dose. Enhance the image contrast.
Patient Couch: Consists of a support referred to as couch top (cradle), made from carbon fiber. Pedestal houses the mechanical and electronic components that facilitate vertical and longitudinal movement.

2.3.2.2 The Computer:

Large capacity computer, Microprocessor or array processor Cost 1/3 of the total cost. (D.karthikeyan, deepachgu,2005) .

2.3.4 Helical CT Angiography: Principles, Techniques:

Computed tomographic (CT) angiography has been improved significantly with the introduction of four- to 64-section spiral CT scanners, which offer rapid acquisition of isotropic data sets. A variety of techniques have been proposed for postprocessing of the resulting images. The most widely used techniques are multiplanar reformation (MPR), thin-slab maximum intensity projection, and volume rendering. Sophisticated segmentation algorithms, vessel analysis tools based on a centerline approach, and automatic lumen boundary definition are emerging techniques; bone removal with thresholding or subtraction algorithms has been introduced. These techniques increasingly provide a quality of vessel analysis comparable to that achieved with intra-arterial three-dimensional rotational angiography. Neurovascular applications for these various image post processing methods include steno-occlusive disease, dural sinus thrombosis, vascular malformations, and cerebral aneurysms. However, one should keep in mind the potential pitfalls of these techniques and always double-check the final results with source or MPR imaging. (Radiographics.rnsa.org,2011).

In recent years, rapid advances in computed topographic (CT) technology and image post processing software have been made. CT angiography

was improved substantially by increasing scan speed and decreasing section thickness and emerged as a powerful tool in neurovascular imaging. Nowadays, spiral CT systems with acquisition capabilities of up to 64 sections per gantry rotation are introduced in clinical practice. Gantry rotation times decreased to 0.33 second, and section widths of 0.5–0.6 mm are available. Assessment of vascular studies based on axial images alone is not straightforward; two-dimensional (2D) and three-dimensional (3D) visualization methods are routinely employed to create images comparable to those acquired with catheter angiography. In the emergency situation (stroke or subarachnoid hemorrhage), a robust and fast imaging technique capable of answering all vital clinical questions and allowing clear therapeutic decisions is mandatory. Optimal image quality depends on two factors: CT angiography technique (scan protocol, contrast material injection protocol, image reconstruction methods) and data visualization technique. (Radiographics.rnsa.org,2011).

2.3.4.1 Technique of Multi detector CT Angiography

An essential prerequisite for successful post processing is good quality of the acquired imaging data. While the short arteriovenous transit time in neurovascular applications makes short scan times preferable, the small caliber of cervical and intracranial vessels requires the highest spatial resolution in all three dimensions. (Radiographics.rnsa.org,2011).

2.3.4.2 Influence of Scan Speed:

For evaluation of the basal intracranial arteries, a scan range of approximately 100 mm needs to be covered. With four–detector row CT at a collimated section width of 1 mm, a pitch of 1.5, and a gantry rotation time of 0.5 second, this volume can be covered in about 9 seconds. Assuming a cerebral transit time of about 5 seconds, this is not fast enough to avoid venous overlay. With 16–detector row CT at a collimated section width of 0.75 mm, a pitch of 1.5, and a rotation time of 0.5 second, the same range can be covered in 3 seconds, well beyond the arteriovenous transit time. Examination of the whole length of the carotid arteries from the aortic arch to the circle of Willis requires a scan range of approximately 250 mm. With the above-mentioned scan parameters, the scan time would be 21 seconds for four–detector row CT, 7 seconds for 16–detector row CT, and 4 seconds for 64–detector row CT (64 × 0.6 mm, pitch of 1.3, 0.33-second rotation time). The latter protocol allows contrast phase-resolved imaging. (Radiographics.rnsa.org, 2011).

2.4 Contrast Material Injection

Short scan times require short contrast material injection. The injection protocols need to be simple and standardized to guarantee excellent and reproducible results on a 24-hour basis. To deliver an appropriate amount of iodine, injection rates of 4–5 mL/sec and highly concentrated contrast medium (iodine, 350–370 mmol/mL) are preferable. The utility of the contrast material bolus can be increased if a saline bolus is appended. Flushing of the veins reduces streak artifacts due to beam hardening, especially at the thoracic inlet. Individual timing of contrast material

injection (bolus tracking or test bolus injection) is mandatory to take advantage of phase-resolved image acquisition.

To individualize the timing of contrast material injection, automatic bolus tracking techniques (Smart Prep, CARE Bolus, and Sure Start) can be employed. These techniques are fast and easy to use and require only a single contrast material injection. The disadvantage is that a large target vessel for monitoring the contrast material arrival is required, and an additional delay for table movement and patient instruction is necessary.

Test bolus injection is the alternative to assess the individual circulation time. Its major advantage is that it provides information about the timing of both arterial and venous enhancement in the vessels of interest. The individual start delay can be optimized by placing the scan between the arterial peak and venous contrast material upslope. Table movement and patient instructions can be performed prior to the optimal image acquisition window. The disadvantage is the necessity for an additional injection of about 10 mL of contrast agent (10%–20% increase of total amount). (Radiographics.rnsa.org,2011).

2.5 Radiation Quantities and Unit:

The unique radiation exposure conditions that exist in computed tomography (CT), during which thin slices of the patient are irradiated by a narrow, fan-shaped beam of x rays emitted from the x-ray tube during its rotation around the patient, have required the use of special dosimeter techniques to characterize the radiation doses to patients and to monitor CT system performance. This section describes the basic dosimeter quantities used to indicate patient doses during CT. (Robinjwilks, 1981).

2.5.1 Absorbed dose:

The fundamental quantity for describing the effects of radiation in a tissue or organ is the absorbed dose. Absorbed dose is the energy deposited in a small volume of matter (tissue) by the radiation beam passing through the matter divided by the mass of the matter. Absorbed dose is thus measured in terms of energy deposited per unit mass of material. Absorbed dose is measured in joules/kilogram, and a quantity of 1 joule/kilogram has the special unit of gray (Gy) in the International System of quantities and units. (In terms of the older system of radiation quantities and units previously used, 1 Gy equals 100 rad, or 1mGy equals 0.1 rad.). (Robinjwilks, 1981).

2.5.2 Equivalent dose:

The biological effects of an absorbed dose of a given magnitude are dependent on the type of radiation delivering the energy (i.e., whether the radiation is from x rays, gamma rays, electrons (beta rays), alpha particles, neutrons, or other particulate radiation) and the amount of radiation absorbed. This variation in effect is due to the differences in the manner in which the different types of radiation interact with tissue.

The variation in the magnitude of the biological effects due to different types of radiation is described by the "radiation weighting factor" for the specific radiation type. The radiation weighting factor is a dimensionless constant, the value of which depends on the type of radiation. Thus the absorbed dose (in Gy) averaged over an entire organ and multiplied by a dimensionless factor, the radiation weighting factor, gives the equivalent dose. The unit for the quantity equivalent dose is the sievert (Sv). Thus,

the relation is Equivalent dose (in Sv) = absorbed dose (in Gy) x radiation weighting factor

In the older system of units, equivalent dose was described by the unit rem and 1 Svequals 100 rem or 1 mSv equals 0.1 rem. For x rays of the energy encountered in CT, the radiation weighting factor is equal to 1.0. Thus, for CT, the absorbed dose in a tissue, in Gy, is equal to the equivalent dose in Sv. (Robinjwilks, 1981).

2.5.3 Effective dose

The risk of cancer induction from an equivalent dose depends on the organ receiving the dose. A method is required to permit comparison of the risks when different organs are irradiated. The quantity "effective dose" is used for this purpose. The effective dose is calculated by determining the equivalent dose to each organ irradiated and then multiplying this equivalent dose by a tissue-specific weighting factor for each organ or tissue type. This tissue- or organ-specific weighting factor accounts for the variations in the risk of cancer induction or other adverse effects for the specific organ. These products of equivalent dose and tissue weighting factor are then summed over all the irradiated organs to calculate the "effective dose." (Note that effective dose is a calculated, not measured quantity.) The effective dose is, by definition, an estimate of the uniform, whole-body equivalent dose that would produce the same level of risk for adverse effects that results from the non-uniform partial body irradiation. The unit for the effective dose is also the sievert (Sv). (Robinjwilks, 1981).

2.6 CT Dose Descriptors:

The dose qualities used in projection radiography are not applicable to CT for three reasons

First: The dose distribution inside the patient is different from that of conventional radiologram, in case of CT, as a consequence of scanning procedure that equally irradiates from all direction.

Second: Scan procedure using narrow beams along the longitudinal z-axis of the patient.

Third, the situation with CT, unlike with conventional projection radiography is further complicated by the circumstances in which the value to be imaged is not irradiated simultaneity. This often led to confusion about what dose from a complete series. As a consequence, dedicated dose quantities that account for these peculiarities are needed the computed tomography dose index (CTDI) and the dose – length product (DLP) and effective dose. (Robinjwilks, 1981).

2.6.1 Computed Tomography Dose Index (CTDI):

CTDI is the fundamental CT dose descriptor the CTDI unit is milligray (mGy) is derived from the dose distribution a long a line that parallel to the axis of rotation for the scanner (=z axis) and is recorded for a single rotation of x-ray source CTDI is equivalent of dose value inside the irradiated slice (beam), CTDI therefore describes the summation of all dose contribution a long the z-axis.

$$CTDI = \frac{1}{N.h_{col-x}} / D(z).dz$$

D2 = Value of the dose at a given location

z_1 and $N.h_{col}$ = Nominal value of the total collimation (beam width) that use for acquisition.

The CTDI becomes obvious from the total dose profile of scan series with the average level of the total dose profile which is called multiple san arrange dose (MSAD) – (Shope 1981).

CTDI and MASD are exactly equal of the table feed (TF) is equal to the nominal beam width $N.h_{col}$

$$MSAD = \frac{1}{P} (CTDI)$$

Each pair of CTDI (Central and peripheral) can be combined into a single are named weighted CTDI ($CTDI_W$):

$$CTDI_W = \frac{1}{3} CTDI_c + \frac{2}{3} CTDI_p$$
$$xyz \qquad xyz$$

If pitch – related effected on the radiation exposure have already been taken into account at level of local dose (i.e, CTDI) a quantity named volume CTDI ($CTDI_{vol}$) is define (1EC 2001).

$$CTDI_{vol} = \frac{CTDI_W}{P}$$

$CTDI_{vol}$ therefore represent the average dose for a given scan volume, and it used as the dose quality that is displayed at operator's console of a newer scanners. (Robinjwilks, 1981).

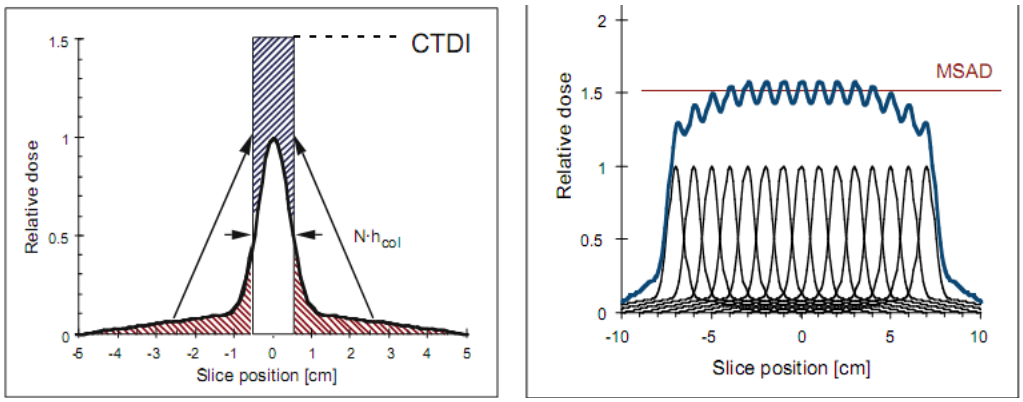

Figure 2.7: CTDI in single and multi-detector CT.
(Bethesda1976).

2.6.2 Dose – Length Product (DLP) Unit (mGy-cm):

DLP = CTDIW.L (mGy-cm). DLP takes both the intensity represented by $CTDI_{vol}$ and the extension (Represented by scan length) of an irradiation into account. DLP increases with number of slices (With the length of

irradiated body section), DLP is the equivalent of the dose area product (DAP) in projection radiography.

In sequentional scanning, the scan length is determined by beam width $N.h_{col}$ and number of the table feed (TF). While in spiral scanning the scan length only depends on the number (n) of rotations and table feed TF (Robinjwilks, 1981).

$$L = n.\ TF = \frac{T}{t_{rot}}.\ P.\ N,h_{col}$$

T = Total scan time.

t_{rot} = Is rotation time.

P = Is pitch factor.

In sequentional scanning the scan length is equal to the range from the benign of the first slice until the end of the last slice (IMPACT Report2005).

$$DLP_{exam} = \sum_i DLP$$

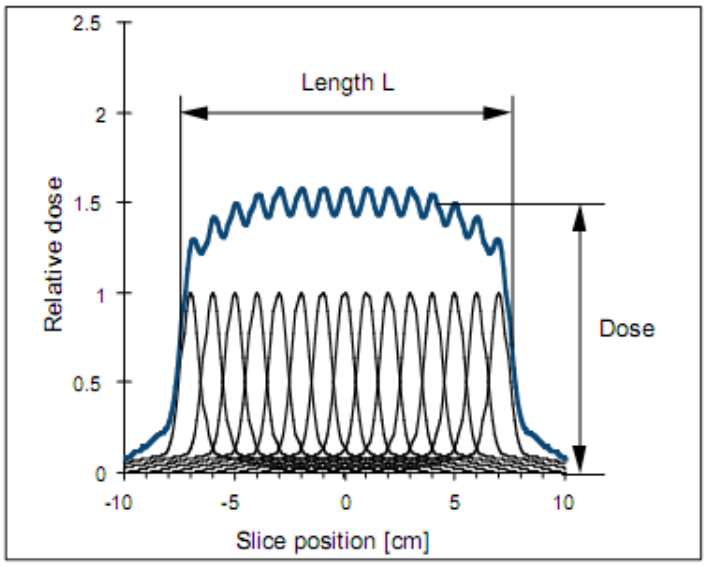

Figure 2.8: Dose length product in CT

(Bethesda1976).

2.6.3 Automatic Dose Control Device:

Newer scanning is equipped with means that automatically adapt the mAs settings to the individual size and shape of the patient.

Automatic dose control systems offer up to four different functionalities that can be use either alone or in combination.

AEC, which accounts for the average attenuation of patient's body region that is to be scanned. Information on the patient's attenuation properties are derived from the scan projection radiogram (SPR) usually recorded prior to the scan for planning purposes. (Hausleiter et al.2009).

2.6.4 Dose Display:

Newer scanners must be equipped with a dose display. Only the display of $CTDI_{vol}$ is mandatory many scanners also show DLP, either per scan series or both per scan series and per exam.

The dose display can be used for purposes of dose optimization. $CTDI_{vol}$ can be used as a fair estimate for the dose to organs that are entirely located in the scan range. Many dose recommendations are given interns of ($CTDI_W$); in order to allow for comparison, the pitch correction involved in $CTDI_{vol}$ must be reverted by multiplying $CTDI_{vol}$ by the pitch factor. Until now, the dose values for examination carried out in body scanning mode has always been based on body-CTDI regardless of patient size. In pediatric CT examinations, the displayed figures should be multiplied by 2 for children and by 3 for infants in order to give a realistic estimate of patient dose. (Hausleiter et al.2009).

2.7 Scan Parameter:

2.7.1 Tube current – Time product (Q):

As in conventional radiology, a linear relationship exists between the tube current – time product and dose. The mAs product Q for a single sequential scan is obtain by multiplying the tube current I and exposure time t; in spiral scan mode, Q is the product of the tube current I and rotation time t_{rot}. The tube current – time product is often used as a surrogate for the patient dose (i.e. CTDI) with the advent of multi-slice scanners, additional confusion arose due to the introduction of a different (pitch – correct mAs notation 'effective mAs', or mAs per slice).
Tube current – time product should be adapted to characteristic of the scanner, the size of the patient and the dose requirement. (Hausleiter et al.2009).

2.7.2 Tube potential (kVp):

In conventional projection radiology, when the tube potential is increased, both the tube output and the penetration power of the beam are improved, while the image contrast is adversely indicated. Increased tube potential are applies in order to ensure short exposure times or to reduce patient dose. In CT, increased tube voltages are used preferentially for improvement in tube loading and image quality, the consequence of variation in kV cannot easily be assessed. The relationship between dose and tube potential U is not linear, but rather of on exponential nature which varies according to the specific circumstances.
Decreasing tube current by 50% will essentially decrease radiation dose by 50%. 80 kV instead of 120 kV would allow reduction of the patient dose by almost a factor of two without sacrificing image quality.
Tube potential other that 120 kV should be considered only in the case of: Obese patients in whom mAs cannot be further increased: use higher kV setting. Slim patients and pediatric CT, when mAs cannot be further reduced: uses lower kV setting.CT angiography with iodine: use lower

kV setting. Variation in tube potential should not be considered for pure dose reduction purposes except in the case of CT angiography. (Hausleiter et al.2009).

2.7.3 Slice collimation (h_{col}) and slice thickness (h_{rec}):

With single – slice CT (SSCT), the slice collimation h_{col} used for data acquisition and the reconstructed slice thickness h_{rec} used for viewing purposes were identical. So there was no need to distinguish between them. With MSCT, the slice collimation (e.g. 0.75mm) and the reconstructed slice thickness h_{rec} (e.g. 5 mm) are usually different. Frequently, the selection of h_{rec} is made with aspect to MPR purposes. As reduced slice thickness is associated with increased image noise, this may have a significant impact on patient dose as express by the Brook's formula. The slice collimation should be selected as compatible with aspects of over teaming over ranging, total scan time and tube poseur. Viewing should be preferentially be mad with thicker slabs thereby reducing image noise and other artifacts, thinner skips should only be used if partial volume effect is of importance.

Except for very narrow slices, there should be no need for any increase in dose settings on reduction of slice thickness. (Hausleiter et al.2009).

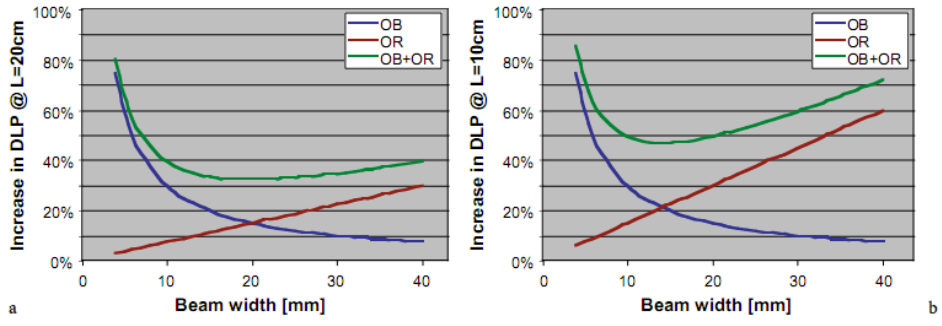

Figure2.9: Relationship between beam width and dose length product (Hausleiter et al.2009).

2.7.4 Pitch:

Defined as tube distance travelled in one 360^{o} rotation/total collimated width of x-ray beam. Is inversely proportional to patient dose (Longer pitchs lower radiation dose). The relationship between pitch and radiation dose is linear, specifically increasing the pitch from 1.0 – 1.5 will reduce the dose by 33%. (Hausleiter et al.2009).

2.7.5 Gantry rotation time:

Decreasing gantry rotation time decreases radiation dose in linear fashion. The faster the gantry rotation, the lower the dose increasing the cycle speed of rotation from 1.0–0.5 seconds per 360^{o} rotation reduced the dose essentially by 50%.

Pitch (P): With SSCT scanners, scanning at increased pitch settings primarily severe to increase the speed of data acquisition, MSCT scanners make use of a spiral interpolation scheme that is different from SSCT. Scanners that make use of effective mAs (mAs per slice) concept not only keep slice profile width, but also image noise constant when pitch change. Pitch setting with MSCT scanners should be made exclusively with respect to scan speed, spiral artifacts and tube power, dose consideration no longer play a role it scanners that employ effective mAs are used or if (Electrical) mAs is adapted to pitch to achieve constant image noise. (Hausleiter et al.2009).

2.7.6 Object diameter (d) or patient (m):

Patient, size, although not a parameter to be selected at the scanner's console. In order to avoid unnecessary over exposure, the mAs must be intentionally adapted by the operator unless AEC-like devices are available.

Relative & body weight + 5kg

mAs setting should be adapted to patient size in more gentle way (Factor of per 8-cm change in diameter).

Preferentially, AEC systems that measure rather than estimate patient absorption should be used, provided that their algorithm makes use of this more gentle mAs adjustment.

Manual adjustment using a set of patient – weight adapted protocols based on regular formula.

Relative mAs & body weight + 5kg

Should be applied instead

For head examinations, mAs adaptation should not be made with respect to patient weight, but to patient age. (Hausleiter et al.2009).

2.8 Examination Parameters:

2.8.1 Scan Length (L):

CTDI is almost in dependent of length of the scanned body section. DLP, and effective dose, both increase in proportional to the length of body section. Therefore, limiting the scan length according to the clinical needs is essential. For each patient the scan length should be selected individually, based on the scan projection radiography that is generally made prior to scanning for the purpose of localization, as should be kept as short as necessary. Moreover a reduction in the scan range should be considered in multi-phase examination and follow-up studies. (Hausleiter et al.2009).

2.8.2 Number of scan series (n_{ser}):

In CT terminology, a scan series is usually referred to as a series of consecutive sequential scan or one complete spiral scan.

The number of scan series (Phase) should be kept as low as necessary. This holds true particularly for liver examination, where studies with up

to six different phase are sometimes recommended in literature. (Hausleiter et al.2009).

2.8.3 Number of rotation in dynamic CT studies (n):

In dynamic CT studies, e.g. in CT fluoroscopy or in perfusion studies, a multiple number of scans is made at the same position. Therefore, it is meaning full to sum up the local doses.

The doses applied in dynamic studies depend on two factors, i.e. the CTDI per rotation and number of rotations. As perfusion studies are regularly made with administration of contrast agents, the benefits of reduced K.V setting should be used to reduce the dose settings. The number of rotation can be kept low by limiting the total length of the study, by reducing the image acquisition rate or by intermitting the procedure. Dynamic CT studies should be made with the lowest dose setting, the most narrow beam width, the shortest length and the smallest images rate that is compatible with clinical needs of examination. (Hausleiter et al.2009).

2.9 Previous studies:

Jörg Hausleiter et al (2009), made a study about estimated of Radiation Dose Associated With Cardiac CT Angiography. To estimate the radiation dose of CCTA in routine clinical practice as well as the association of currently available strategies with dose reduction and to identify the independent factors contributing to radiation dose. The median DLP of 1965 CCTA examinations performed at 50 study sit was 885 mGy × cm (interquartile range, 568-1259 mGy × cm), which corresponds to an estimated radiation dose of 12 mSv (or 1.2 × the dose of an abdominal CT study or 600 chest x-rays). A high variability in DLP was observed between study sites (range of median DLPs per site, 331-2146 mGy × cm).

Also in (2009) Dr J Rixe et al made a comparison between Radiation dose estimated of dual-source, 16-slice and 64-slice CT slice for non-invasive coronary angiography. Retrospective data analysis was performed on 292 patients: 56 patients were examined with 16-slice MDCT, 38 patients with 64-slice MDCT and 202 patients using DSCT. The effective dose (ED) estimates were calculated for all patients from the dose–length product and the conversion factor k (0.017 mSv/mGy/cm), as recommended by current guidelines. The mean (SD) ED for patients examined by 16-slice MDCT was 9.8 (1.8) mSv, for 64-slice MDCT 8.6 (2.8) mSv and for DSCT 11.4 (7.2) mSv. With a protocol of 100 kV tube voltage and 110 ms ECG pulsing window the mean (SD) ED was 3.8 (1.7) mSv for DSCT scanning. When DSCT with a tube voltage of 100 kV was used, a significant inverse correlation between heart rate and radiation dose exposure was found.

Fatima (2011), had estimated Radiation Dose Associated with Cardiac CT Angiography in 32 patients. A cross-sectional, international, multicenter, linear regression analysis was used to identify independent predictors associated with dose. Dose-length product (DLP) of CCTA. The DLP of of chest is929.625 mGy × cm , for abdomen 1672.7 mGy × cm J and limbs 7386.81 mGy × cm.

Another study by Ali (2012) in 50 patients the DLP of chest is 1878.7 mGy × cm. for abdomen is 3174.1 for limbs is 2370.5 mGy × cm.

Also Manal (2012) made a study in 50 patients DLP of chest is 1281.80 mGy × cm.,for abdomen is 4166.00 mGy × cm.,and limbs is 4378.20 mGy × cm.

Chapter Three

Materials and Methods

This study is analytic clinical base study. The data were collected from Royal Scan diagnostic Center, Khartoum, Sudan, in the period September 2015- December 2015 The data was collected randomly from patient undergoing CTA with different clinical indications.

3.1 Materials:

3.1.1 Patients:

A total of 50 patients referred to Royal Scan diagnostic Center in the period of study. The work performed to evaluate the effective dose of patient undergoing to CTA examination .The patients were distributed through different angiographic procedures.

3.1.2 Machine used:

The CT images were made using (TOSHIBA aquilion 64 slices 2010) CT scanner. The scan parameter (3mm slice, 120 kvp,225 mAs). And with using the electronic calliper with in the scanner the following diameters were measured.

3.2 Methods:

3.2.1 Patient Preparation:

The patient should be fasting at least 8 hours before the exam for all CTA investigations and ensure that the patient understands the procedure, particularly breath-holding techniques.

The patient history should be obtained to identify patient with history of iodine allergy renal dysfunction, cardiac disease, and asthma .steroid premedication should be administered to those patients with a history of iodine allergy or previous reaction to iodinated contrast agent.

For CCTA procedures, special preparation is done for high image quality the highest image quality of coronary CTA for current generations of 16- and 64-slice MDCT scanners can be achieved at low heart rates (<65 beats per minute).

Therefore, aggressively reducing a patient's heart rate before a scan is advised for patients with a heart rate of more than 70 beats per minute. Patients are positioned on the CT examination table in the supine position. Arms positioned comfortably above the head, lower legs supported for chest, abdomen, and lower limb. Intravenous access via a large intravenous line is necessary to ensure easy injection of the viscous contrast agent at a flow rate of 5 mL/s. except in very obese patients, a flow rate of 4 mL/s usually renders diagnostic image quality as well

3.2.2 The Examination protocol used in CTA:

Initial scan without IV contrast, patient should suspended respiration during scan. Start with scout view to localize start and end position (according to area in question). Starts scan area using thin slice thickness, this sequence without injection of contrast media. After that injected IV contrast medium at a flow rate of 4-5 mL/s, CT images are taken and reconstructed after that post processing technique is applied according to the need.

3.2.3 CT dose evaluation:

The patient dose estimation from CT examination using the Monte Carlo technique requires measurements of CTDI and conversion coefficient data. In theory, the CTDI, which is a measure of the dose from single-slice irradiation, is defined as the integral along a line parallel to the axis of rotation (z) of the dose profile, D(z), divided by the nominal slice thickness,T. In this study, CTDI was obtained from a measurement of dose, D(z), along the z-axis made in air using a special pencil-shaped

ionization chamber (Diados, type M30009, PTW-Freiburg) connected to an electrometer (Diados, type 11003, PTW-Freiburg). The calibration of the ion chamber is traceable to the standards of the German National Laboratory and was calibrated according to the International Electrical Commission standards. The overall accuracy of ionization chamber measurements was estimated to be ±5%. Measurements of CTDI in air ($CTDI_{100}$, air) were made as recommended by the EUR 16262EN based on each combination of typical scanning parameters obtained from the machine. The required organ doses for this study were estimated using normalized CTDI values published by the ImPACT group. For the sake of simplicity, the CTDI100, air will hence forth be abbreviated as $CTDI_{air}$.

Chapter four

4-1 Results:

In this study, a total of 50 patients were examined in Royal Scan Diagnostic Center in Khartoum, the study data are presented in the following graphs and tables

Table 4.1 shows number of patients, age, mAs, scan time, DLP, CTDIvol and Effective dose

Organ	No	Age	mAs	Scan time	DLP	CTDIvol	Effective dose
Renal Angiogram	16	60.18±11.0	10100.50±1295.0	42.89±6.0	3444.7±1022.5	412.6±78.3	51.6±15.3
		45.0-77.0	7041.0-12406.0	32.1-52.1	1199.8-5012.1	256.4-517.9	17.9-75.1
Coronary Angiogram	16	59.2±16.0	8165.9±3137.0	38.2±12.7	2254.1±720.6	721.94±227.8	31.5±10.0
		38.0-82.0	1429.0-15188.0	17.0-65.3	1188.8-3962.7	491.7-1184.4	16.6-55.4
Lower limb Angiogram	18	65.2±12.2	14001.5±2012.1	65.5±9.6	4967.8±1123.0	253.6±95.6	74.5±16.8

		45.0±82.0	**11792.0-19609.0**	**53.2-83.0**	**3357.7-7048.5**	**119.7-475.0**	**50.3-105.7**

Table 4.2: shows Patient Dose parameters: CTDIvol, DLP, and effective dose

Organ	No	CTDIvol (mGy)	DLP(mGy.cm)	Eff.dose(mSv)
Renal Angiogram	**16**	**412.6±78.3**	**3444.7±1022.5**	**51.6±15.3**
		256.4-517.9	**1199.8-5012.1**	**17.9-75.1**
Coronary Angiogram	**16**	**721.94±227.8**	**2254.1±720.6**	**31.5±10.0**
		491.7-1184.4	**1188.8-3962.7**	**16.6-55.4**
Lower limb Angiogram	**18**	**253.6±95.6**	**4967.8±1123.0**	**74.5±16.8**
		119.7-475.0	**3357.7-7048.5**	**50.3-105.7**

Table 4.3: shows Patient exposure parameters: mAs , Slice thickness, and pitch.

Organ	mAs	Slice thickness (mm)	Pitch
Renal angiogram	**7041.0-12406.0**	**3**	**0.73**
Coronary angiogram	**1429.0-15188.0**	**3.5**	**0.53**
Lower Limb	**11792.0--19609.0**	**5**	**0.53**

angiogram

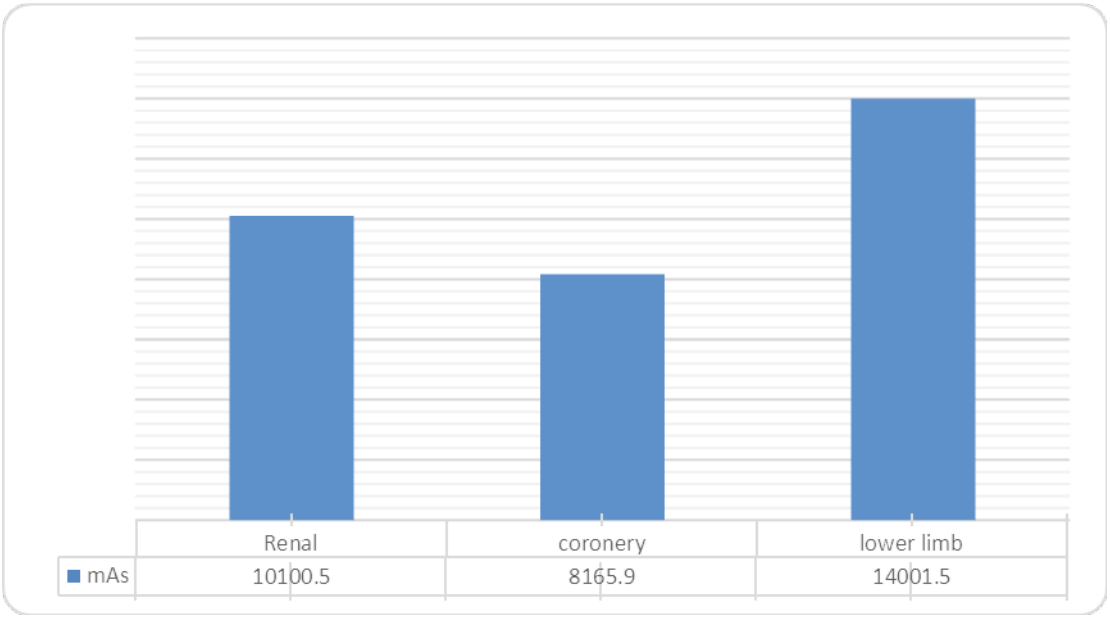

Fig (4.1) shows comparison between mAs in three examinations.

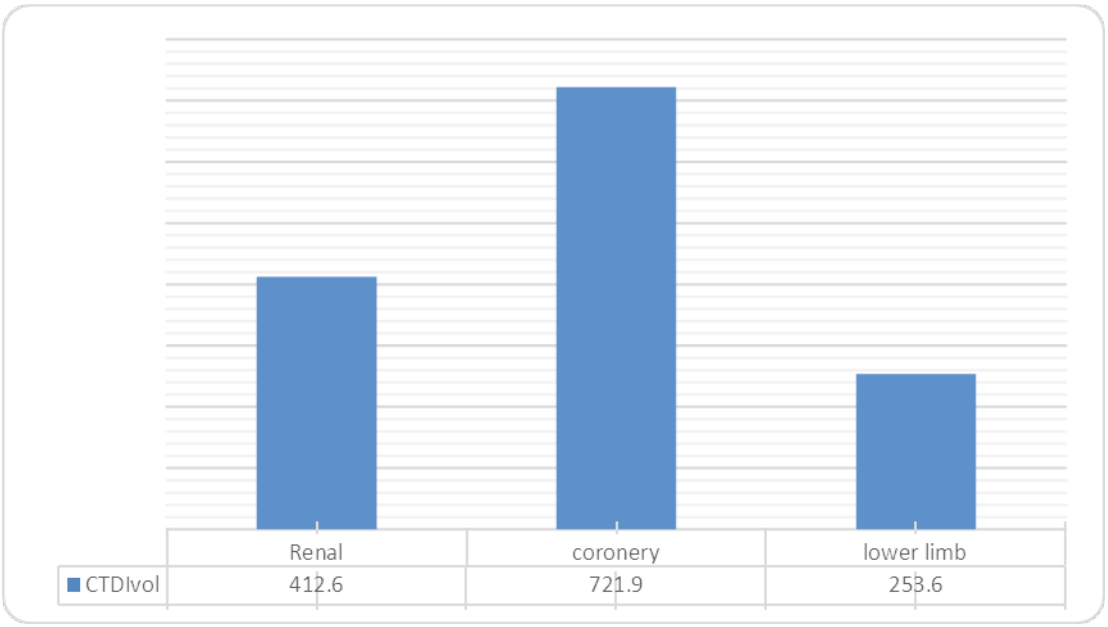

Fig (4.2) shows comparison between CTDI vol in three examinations.

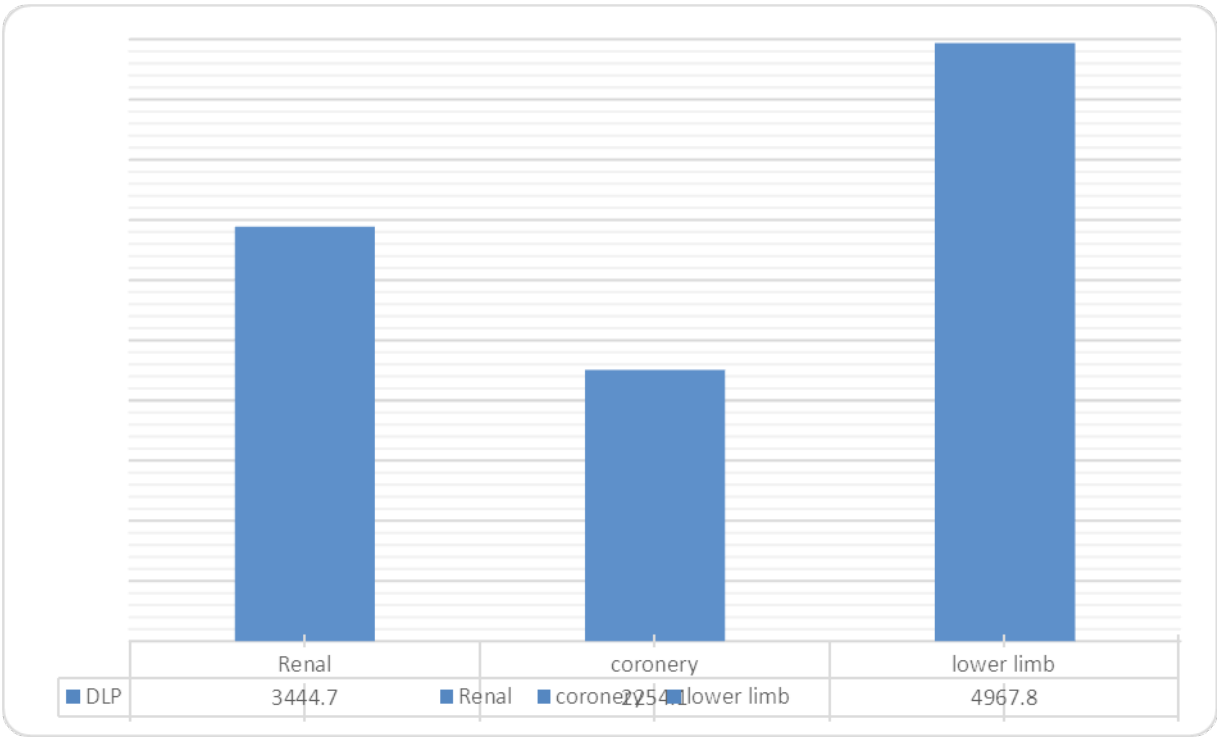

Fig (4.3) shows comparison between DLP in three examinations.

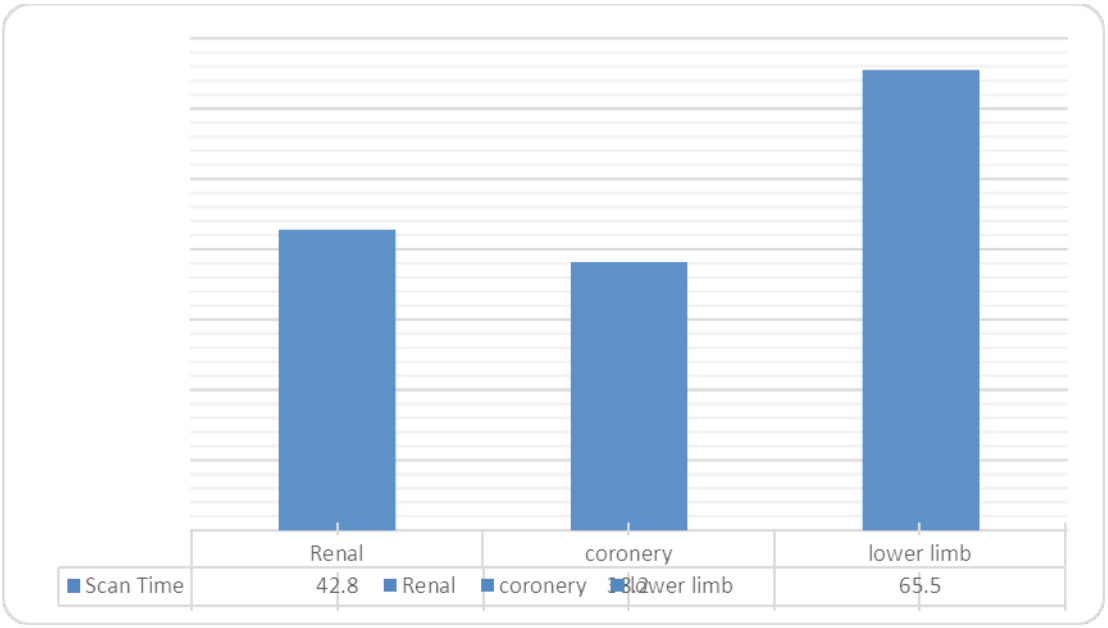

Fig (4.4) shows compare between Scan time in three examination.

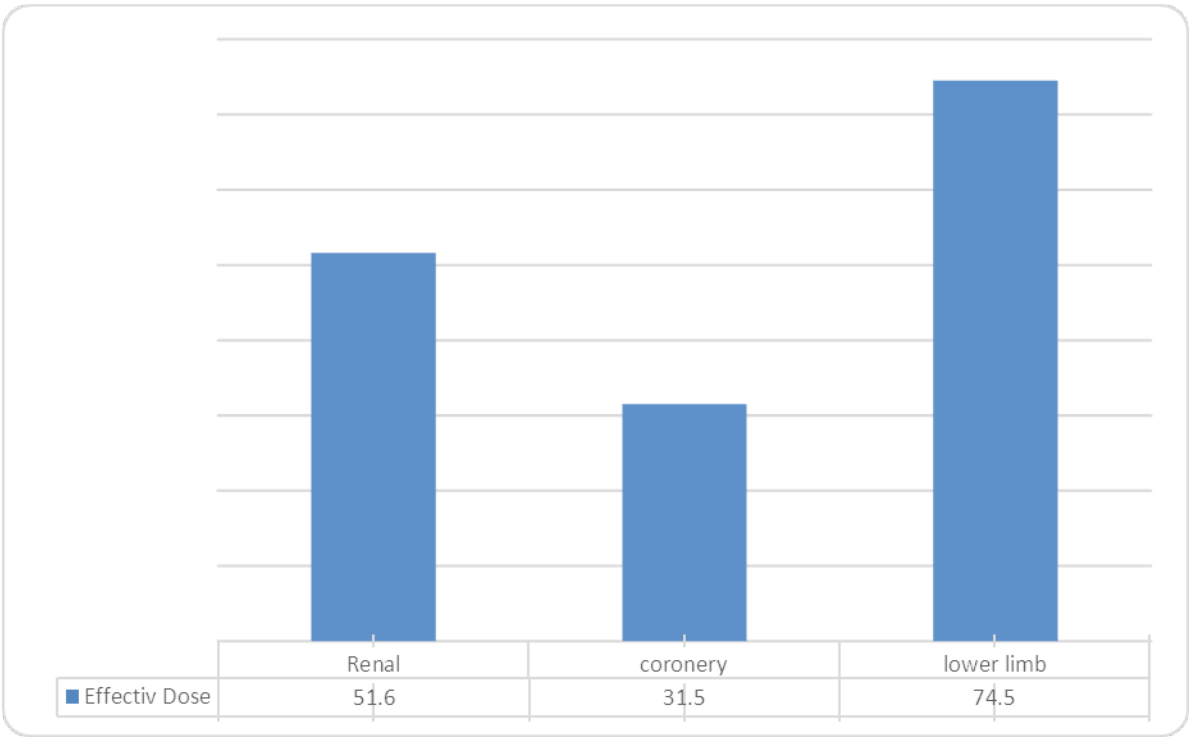

Fig (4.5) shows comparison between effective dose in three examinations.

CORONARY

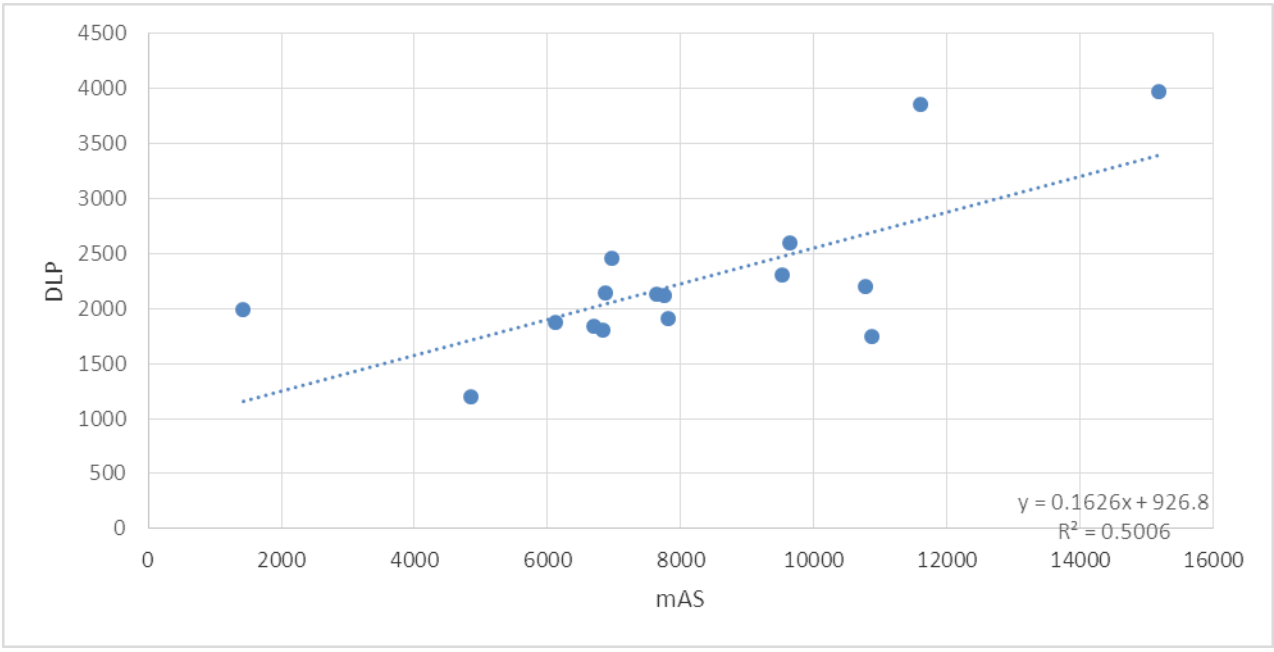

Figure (4.6) A scatter plot diagram shows linear relationship between total mAs and DLP in coronary examination as the total mAs increased the total DLP increased also it was increased by 0.1626x starting from 926.8.

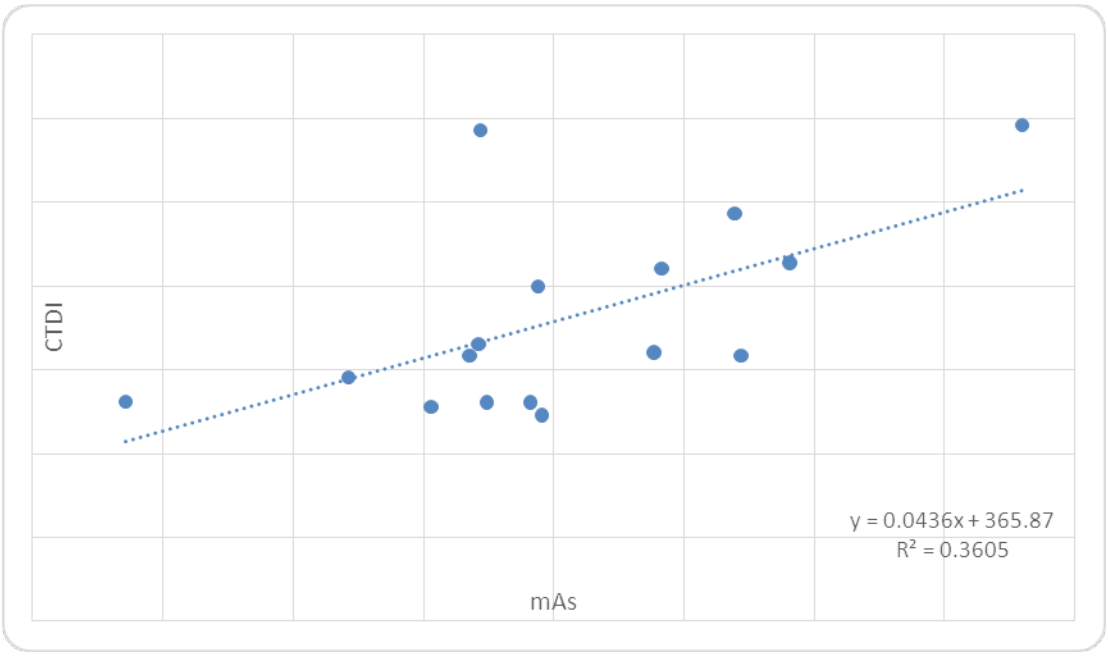

Figure (4.7) A scatter plot diagram shows linear relationship between CTDIvol and total mAs as the total mAs increased the CTDIvol increased also it was increased by 0.043x starting from 365.8.

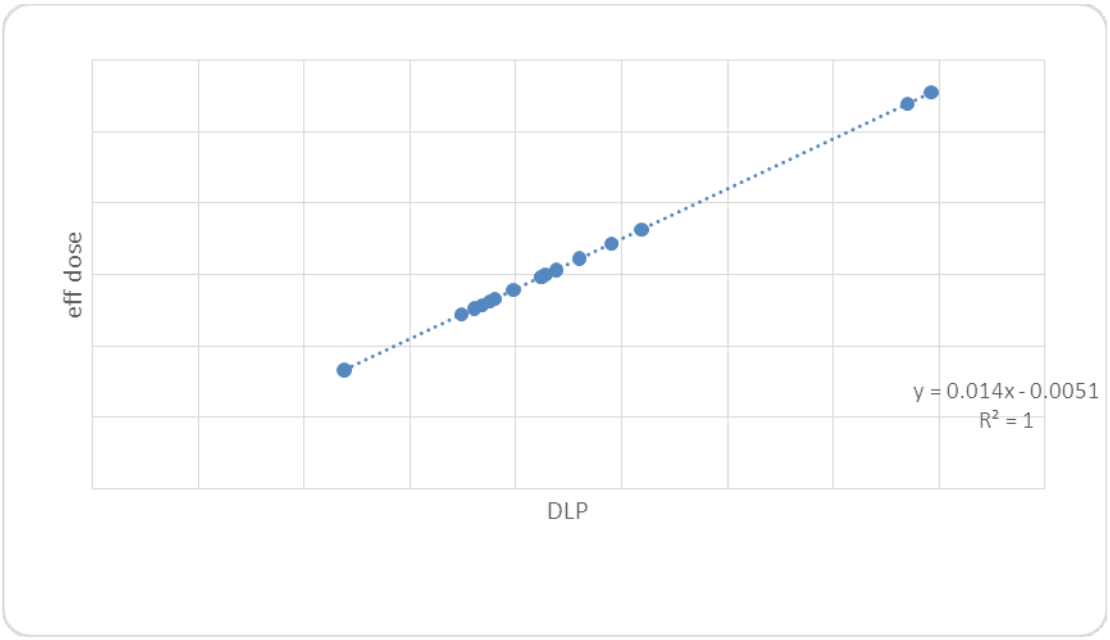

Figure (4.8) A scatter plot diagram shows linear relationship between effective dose and DLP as the DLP increased the effective dose increased also it was increased by 0.014x starting from 0.005.

RENAL

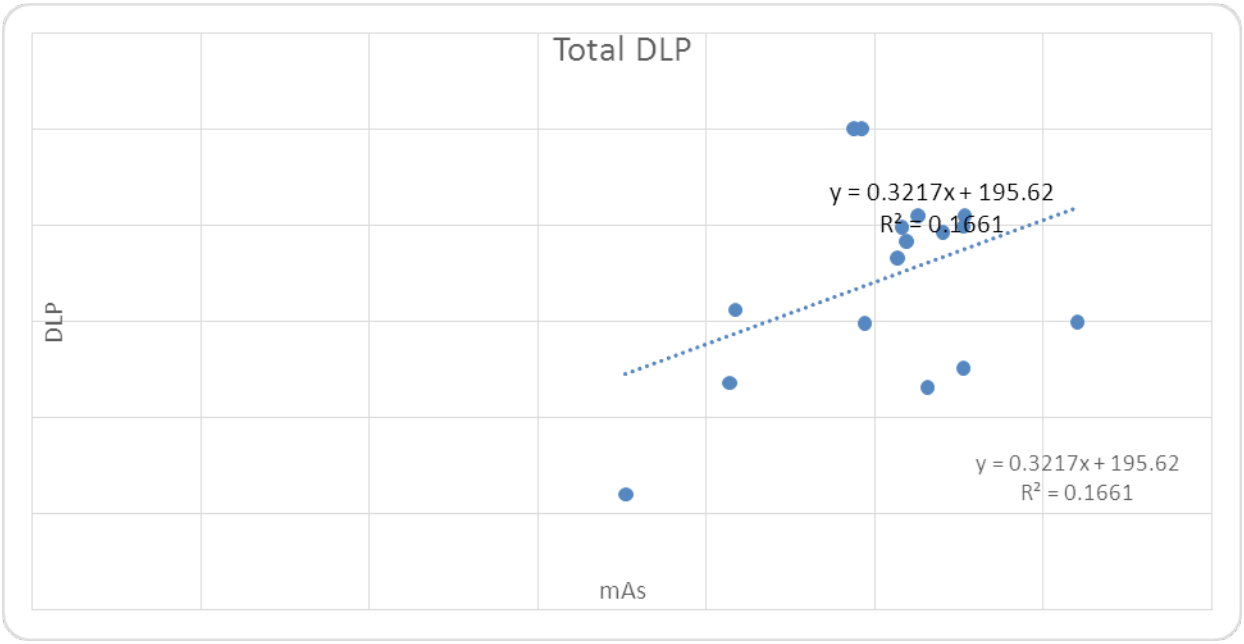

Figure (4.9) A scatter plot diagram shows linear relationship between total mAs and DLP in renal angiography examination as the total mAs increased the total DLP increased also it was increased by 0.3217x starting from 195.62.

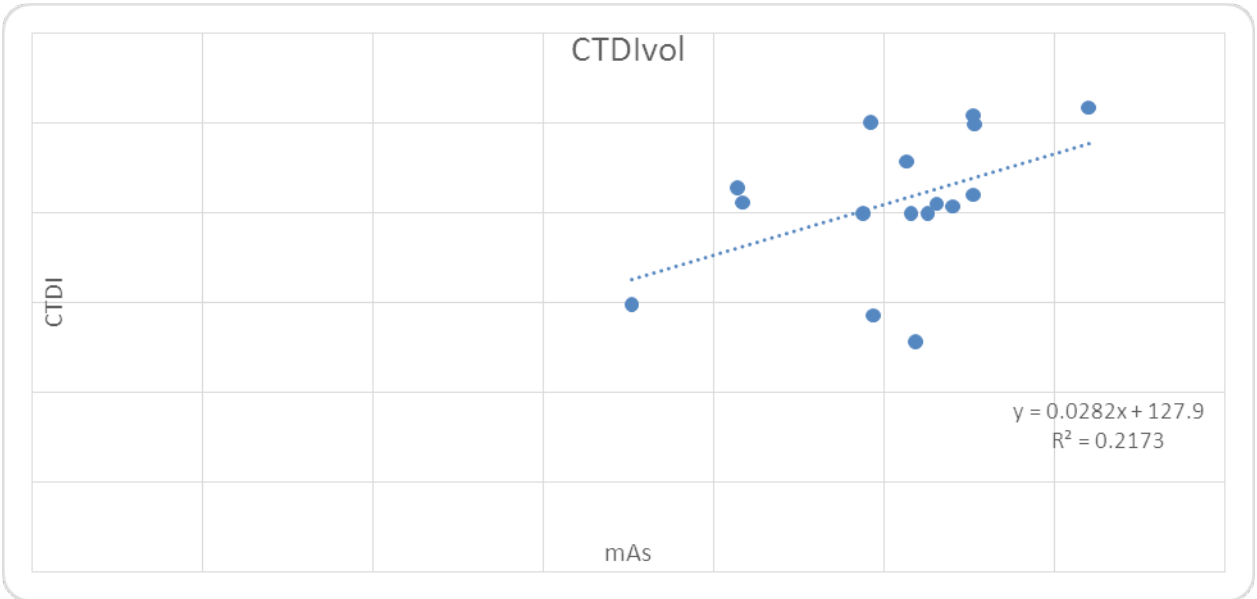

Figure (4.10) A scatter plot diagram shows linear relationship between CTDIvol and total mAs as the total mAs increased the CTDIvol increased also it was increasedby 0.0282x starting from 127.9.

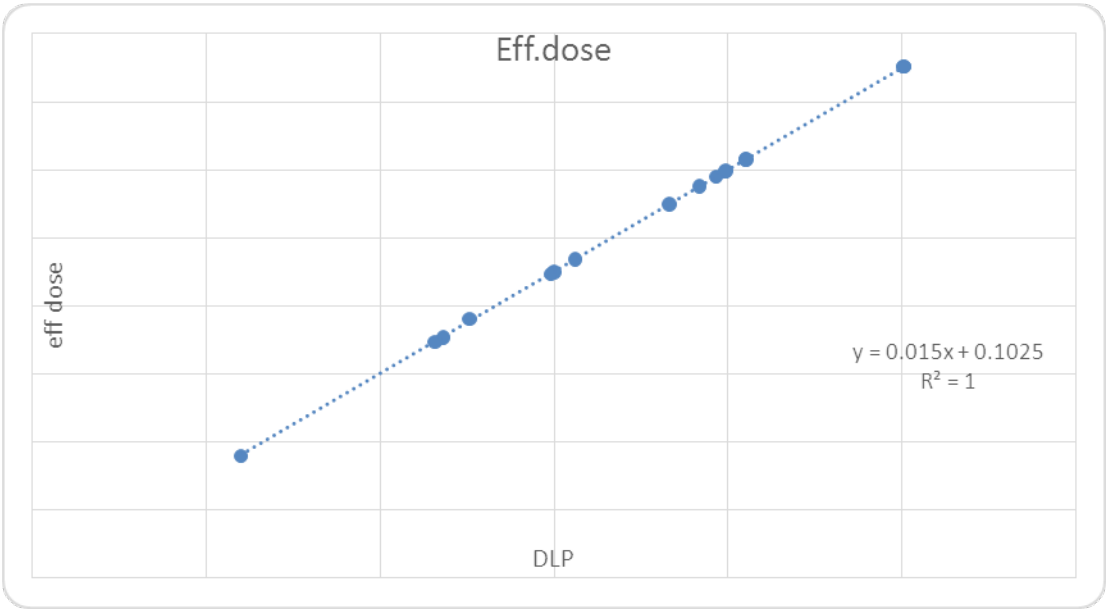

Figure (4.11) Ascatter plot diagram shows linear relationship between effective dose and DLP as the DLP increased the effective dose increased also it was increased by 0.015x starting from 0.1025.

LOWER LIMB

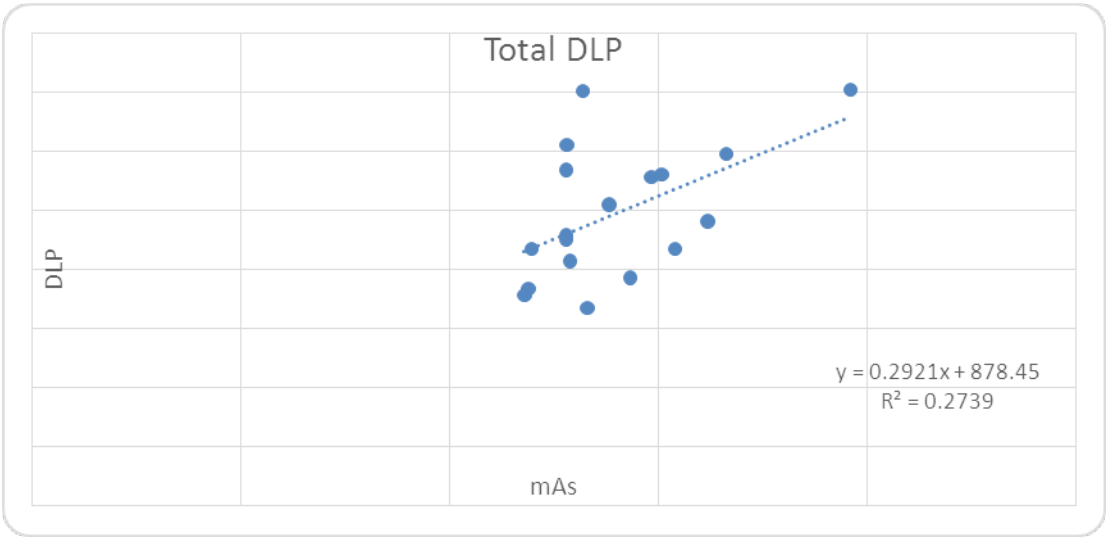

Figure (4.12) A scatter plot diagram shows linear relationship between total mAs and DLP in lower limbs angiography examination as the total mAs increased the total DLP increased also it was increased by 0.2921x starting from 878.45.

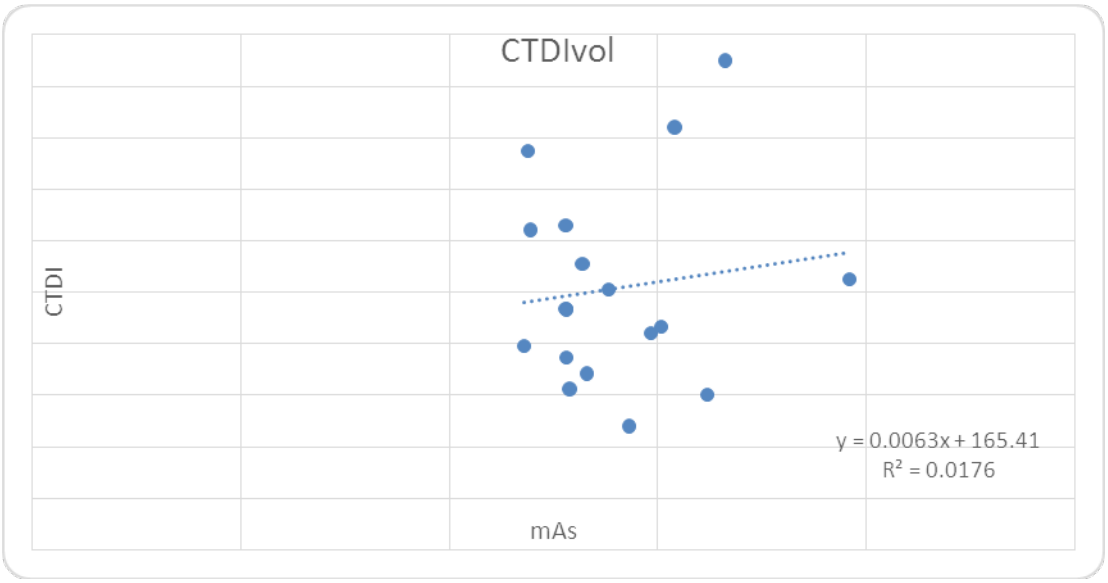

Figure (4.13) A scatter plot diagram shows linear relationship between CTDIvol and total mAs as the total mAs increased the CTDIvol increased also it was increased by 0.0036x starting from 165.41

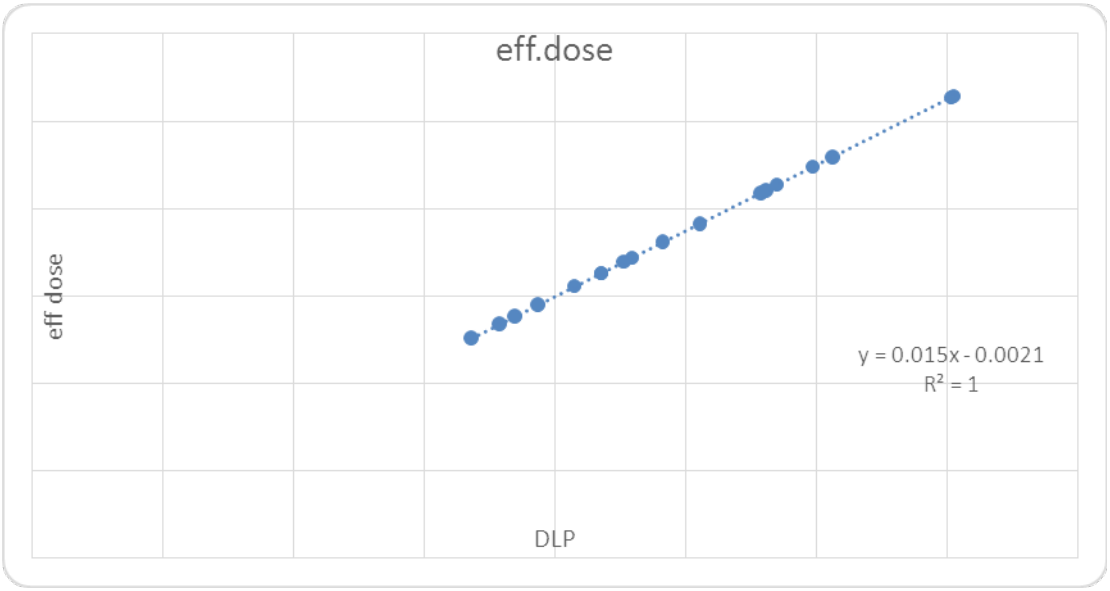

Figure (4.14) A scatter plot diagram shows linear relationship between effective dose and DLP as the DLP increased the effective dose increased also it was increased by 0.015x starting from 0.0021.

Chapter five

Discussion, Conclusion and Recommendations

5.1 Discussion

CT is a versatile and valuable imaging modality in the medical industry. A CT's image quality determines its ability to aid in the care and management of the patient.

Recent technical advancements in CT have resulted in a remarkable growth in the use of CT imaging in clinical practice. Offering faster acquisition, CT scanners have increased availability of CT imaging and expanded its clinical indications. Exposure to high levels of radiation causes cancer. This is a fact well documented and accepted. What remains controversial, however, is whether low levels of ionizing radiation, such as medical x-rays, are definitively carcinogenic. Based on the assumption that there is no lower threshold for carcinogenesis, the authors try to estimate the radiation dose in CTA.

This study shows the age range from (45-77 years), (38-82years) and (45-82years) for renal, coronary and lower limb angiogram respectively. As expected, most of patients are above 40 years old. Also the study shows mAs is high in lower limbs CTA(14001.5±2012.1) and lower in renal CTA (10100.50±1295.0), and very low in coronary CTA (8165.9±3137.0) this variation of mAs could be attributed to different patient size and also differ by the number of sequences in the exam and in the other hand the mean scan time is (42.89±6.0sec) ,(38.2±12.7sec) and (65.5±9.6sec) for renal, coronary and lower limb respectively. The mean CTDIvol (412.6±78.3mGy), (721.94±227.8mGy), and (253.6±95.6mGy) for renal , coronary and lower limb CTA respectively, which is high in

coronary and lower in renal and very low in lower limbs. The mean DLP is(3444.7±1022.5mGy.cm), (2254.1±720.6mGy.cm)and(4967.8±1123.0mGy.cm) for renal, coronary and lower limb respectively this variation between DLP values may result from differences in mAs, the scan length due to differences in age range and pitch values for all ct angiography examinations The study shows The values of DLP in lower limbs is higher than renal and coronary and the DLP value in renal is higher than the DLP value coronary which is same like Fatima(2011) and Manal (2012) and differ from Ali(2012). The mean effective dose (51.6±15.3mSv), (31.5±10.0mSv), (74.5±16.8mSv) for renal, coronary and lower limb respectively. The study show the effective dose of the coronary CTA is (32mSv) which is higher than the CCTA effective dose that estimated by Hausleiter et al (2009) (12mSv) and the CCTA effective dose that estimated by Rixe et al (2009) (8.6mSv).

In general, a linear relationship exists between tube current and radiation dose such that reducing the tube current by 50% will also decrease the dose by half. This can be done by adjustments to gantry rotation cycle time or mA. In addition, the relationship of peak kilovoltage (kVp) and dose is more complex. Basically, lowering the kVp will also lower the dose. With this increase in noise, there is a concomitant decrease in image contrast, but data suggest that Therefore, individual adjustments in CT parameters should be based on several considerations, one of which is scan indication. Large lesions, surveys, or follow-up examinations are considerations for lower dose CT. Parameters should also be adjusted based on the organ system or region scanned.

5.2 Conclusion

The radiation dose was measured in Royal Scan Diagnostic Centre using MSCT Scanner. The radiation dose is higher in the imaging of lower limb CTA than renal and coronary. MSCT scanners 64 slice exposed patients to a high dose. Radiation dose from CT procedures varies from patient to patient. A particular radiation dose will depend on the size of the body part examined, the type of procedure. Typical values cited for radiation dose should be considered as estimates that cannot be precisely associated with any individual patient, examination, or type of CT system. The main dose variations in the same CT unit could be attributed to the different techniques, which justify the important of use radiation dose optimization technique and technologists training. Dose reduction strategies must be well understood and properly used.

5.3 Recommendations

- CT operators must optimize the patient dose to reduce patient cancer risks. Should be uses the best strategies available for reducing radiation dose to allow for mAs reduction in relation to the patient's size and weight , adapted tube current based on patient size (such as weight with fixed tube current scanning
- Clear justification of examination is highly recommended
- Continuous education is highly recommended specially in radiation protection field.
- Avoid repetition of examination (CTA examinations should not be repeated without clinical justification) and imitation of scan length
- Reduction of radiation dose is crucial, bearing in mind the image quality should be considered.
- Requests for CTA scanning must be generated only by qualified medical practitioners and justified by both the referring doctor and the radiologist.
- Further studies are highly encouraged in this field with larger samples and different CT modalities.

References:

Angiogram c:/users/Toshiba /desktop.mht accessed on 15.8.2011

Brenner D, Elliston C, Hall E, Berdon W. Estimated risks ofradiation-induced fatal cancer from pediatric CT. Am J Roentgenol 2001; 176:289-96.

Cunningham, I. A., Judy, P. F. " Computed Tomography." *The Biomedical Engineering Handbook: Second Edition.*Ed. Joseph D. Bronzino Boca Raton: CRC Press LLC, 2000

D.karthikeyan, deepachgu, 2005 step by step CT scan, JAYPEE,first edition

Hausleiter, Tanja Meyer ,Franziska Hermann, Martin Hadamitzky Markus Krebs; Thomas C. Gerber, Cynthia McCullough, Stefan Martinoff Adnan Kastrati, Albert Schömig, Stephan Achenbach. Estimated Radiation Dose Associated With Cardiac CT Angiography. JAMA.. 2009;301(5):500-507.

IMPACT (2005) Report 05016:CT scanner automatic exposure control system, medicine and healthcare products regulatory Agency ,London.

ICRU.Determination of absorbed dose in a patient irradiatedby beam of x or gamma rays in radiotherapy procedure .ICRU report 24,Bethesda Maryland.1976.

Matsuoka, S., Hunsaker, a.r., Gill, R.R., Oliva, I.B., Trotman-Dickenson, B ., Jacobson, F.L., Hatabu, h., Vascular enhancement and image quality of MDCT pulmonary angiography in 400 cases:

Comparison of standard and low kilovoltage settings, Am. J. Roentgenol. 192 6 (Jun. 2009) 1651-1656.

Robinjwilks Bcs phd, principle of radiological physics, Churchill livingstone Edinburgh London Newyourk1981

Stuart G.silverman, Richar H.cohon, CT urography An Atlas.2007.by lippncott Williams and Wilkins.2007.

Valerie C. Scanlon, Tina Sanders 2007 Essentials of Anatomy and Physiology fifth edition.

Willmann JK, Mayer D, Banyai M, et al. Evaluation of peripheral arterial bypass grafts with multi-detector row CT angiography: comparison with duplex US and digital subtraction angiography. Radiology. 2003;229:465-474.

Appendices:

Appendix:1

Sudan University Of Sciences and Technology

College Of Graduate studies

Collecting Data Sheet

No	*Gender*	*Age*	*KVp*	*Total mAs*	*Total scan time*	*Total DLP*	*Total CTDIvol*	*Effective Dose*
1.								
2.								
3.								
4.								
5.								
6.								

Appendix 2:

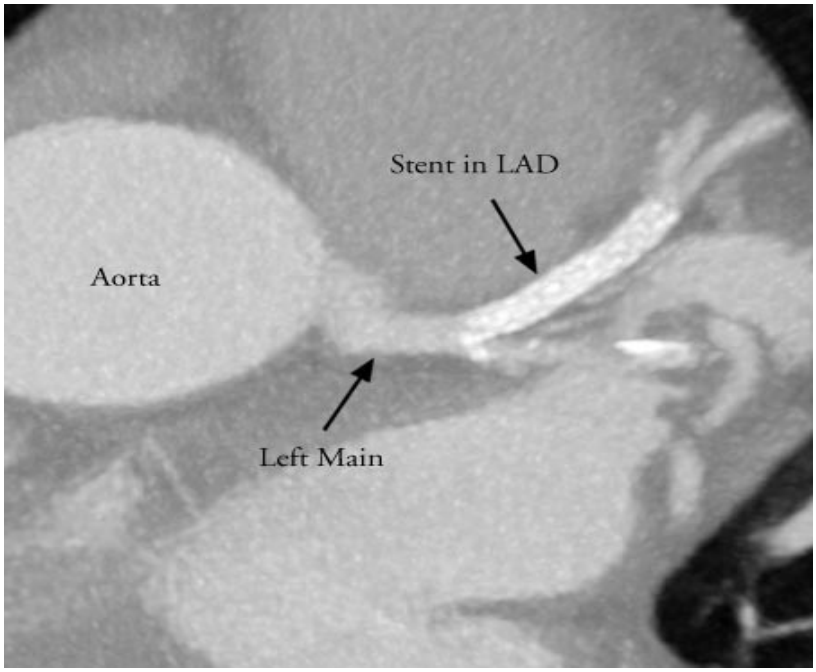

Image 1: for 52 years old male patient coronary CTA shows stent in the left Anterior.

Image 2: for 79 years old male patient, for lower limb CTA shows normal femoral and popliteal arteries.